MASTER'S THESIS IN CHEMISTRY

BONDING IN A TRIAMIDOAMINE-SUPPORTED CHROMIUM(III) CARBONYL

Nkeng Agbor Moses

April 2008

FACULTY OF SCIENCE
Department of Chemistry
University of Tromsø, N-9037 Tromsø

BONDING IN A TRIAMIDOAMINE-SUPPORTED CHROMIUM(III) CARBONYL

Nkeng Agbor Moses

April 2008

Keywords: Chromium, triamidoamine, carbonyl, metal ion, ligand, backbonding, metal-ligand backbonding, Density-Functional Theory (DFT), exchange (XC) functionals, spin occupation.

Abstract: Cr(III) metal ion in low spin triamidoamine-supported chromium(III) carbonyl complex {$[(RN)_3N]CrCO$, **1**} has a unique feature of S=1/2 being unusual for a Cr(III) metal ion, which is high spin with S=3/2 in most complexes and this gives us the basis for this theoretical study. The primary preoccupation has been to determine the electronic ground state and other low-energy state with much emphasis places on the bonding scheme of the conformation obtained at this ground state. DFT calculations elucidated this bonding scheme paying special attention on the Cr-CO metal-ligand π backbonding. Varying the auxiliary ligand (where R= H, CH_3, or C_6H_5) gave significant changes on the results obtained for the metal-ligand backbonding. Their molecular structures were described revealing a trigonal bipyramidal coordination geometry of the chromium center with all structures having Cr-CO bond angle of 180^o being the most stable. Calculations with the highly efficient OLYP, BLYP, OPBE and PW91 DFT functionals with a variation of the spin occupations gave interesting results. An electronic structural analysis of these structures at their different spin occupations indicated that besides the electronic ground state other low-energy states do exist. From a broader perspective, comparison of the results obtained with variation of DFT exchange functionals, spin occupation, auxiliary groups, their respective changes affected on the geometry (bond angles and bond lengths) and on their electronic structures gave a better understanding of the bonding scheme of this complex.

University of Tromsø
2008

ACKNOWLEDGEMENTS

I would like to thank my advisor Prof. Abhik Ghosh for his guidance and for my overall training.

Many thanks are due to my coworkers and friend in the Inorganic chemistry group, including Kolle Thomas, Abraham Alemayehu, Can Capar, and Ingar Wasbotten. Espen Tangen assisted me with software and computation-related issues. Thanks to all of you for being my friends outside of the laboratory.

My deepest thanks go to my entire family for their encouragement, advice, love and financial support. Without their support, I would not have come to this point.

Finally, I am very grateful to God for giving me the strength to face a variety of challenges that I faced during my M. Sc. studies.

Tromsø, April 2008

Nkeng Agbor Moses

TABLE OF CONTENT

CHAPTER 1

INTRODUCTION

1.1 The Problem

Transition metal triamidoamine complexes have attracted much attention in years. The triamidoamine ligand has been found to be a very important ligand for catalysts involved in the reduction of N_2 to NH_3.[1] Part of the uniqueness of the ligand derives from the fact that it creates a "pocket" that helps protect the central metal ion when an appropriate auxiliary group (**h**exa**i**so**p**ropyl**t**erphenyl, HIPT) is attached to the amido nitrogens (the nitrogen that describes the trigonal plain of the structure).

The goal of this project is to understand the bonding in a triamidoamine-supported chromium(III) carbonyl complex {[$(RN)_3N$]CrCO, **1**} (where R= H, CH_3, or C_6H_5).[2] The molecule is shown in Figure 1.1. The carbon monoxide (CO) ligand occupies the top apical position and it is said to be the axial ligand. The isoelectronic molybdenum analogue of this complex is known for its ability to catalyze the reduction of dinitrogen (N_2) to ammonia (NH_3).

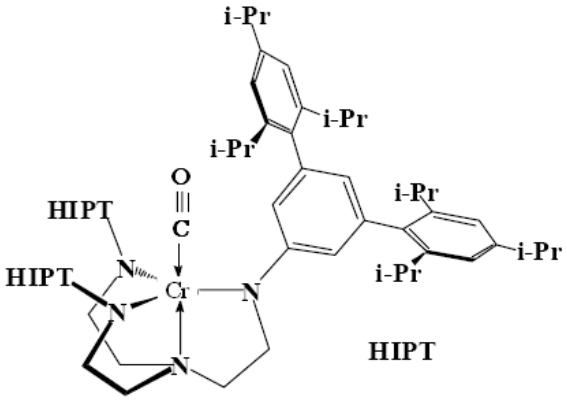

Figure 1.1. Carbonyl complex of Chromium Triamidoamine.[2]

[1] McNaughton, R. L.; Chin, J. M.; Weare, W. W.; Schrock, R. R.; Hoffman, B. M. *J. Am. Chem. Soc.*, **2007**, 129, 3480.
[2] Smythe, N.C.; Schrock, R.R.; Muller, P.; Weare, W. W., *Inorg. Chem*., **2006**, 45, 7111.

The chromium in **1** is Cr(III) with a d^3 configuration. Its unique features are that it is S = ½, unlike most Cr(III) complexes, and that it has only 3 electrons to backbond with the CO ligand. My key goal was to determine the electronic ground state of this complex as well as other low energy states.

Other ligands that could replace CO are dinitrogen (N_2), nitrosyl (NO), cyanide (CN^-), and isocyanide (RCN). These ligands are all π-acceptor ligands.

1.2 The axial ligand

Carbon monoxide (CO) is the most common ligand in organometallic chemistry. It is a very strong field ligand and appears near the end of the spectrochemical series. CO can form a single bond to a metal atom and can also act as a bridging ligand. It can also be bonded to a transition metal in a side on manner where the carbon and oxygen atoms both interact with the same central metal ion. Its chemistry as a ligand has some similarities with other strong field ligands like CN^-, NO^+. They are isoelectronic, each being a 14-electron system. They are all π-acceptor ligands even though they have different π-accepting tendencies. To understand the chemistry of CO as a ligand in this research, we have to take a closer look at its electronic structure and the way it is generally coordinated to a transition metal atom (its bonding).

The CO molecule is formed by three bonds; a σ-orbital and two π-orbital interactions.[3] The σ orbital is made up of diagonal ($2s\text{-}2p_z$) hybrids (which constitute the C-O σ-bond) and are between the carbon and the oxygen atoms (Figure 1.2a). It is believed that the σ lone pair of electrons on the oxygen is less strongly directed than that on the carbon atom. The overlap of the $2p_x$ and $2p_y$ orbitals will then form two π-bonds which will make the triple bond of a free CO giving a total of $(\sigma)^2(\pi_x)^2(\pi_y)^2$.[3] However, the π-bond density (for the antibonding or π* combination) seem to be closer to the carbon atom than to the oxygen atom (Figure1.2b),

[3] Bailar, J. C. Jr.; Emeléus, H. J.; SirNyholm, R.; Trotman-Dickenson, A. F., *Comprehensive Inorganic Chemistry*; Pergamon Press, Oxford, **1973**.

consequently cancelling out the reverse polarity produced by the σ-electrons giving free CO a very low dipole moment.[3]

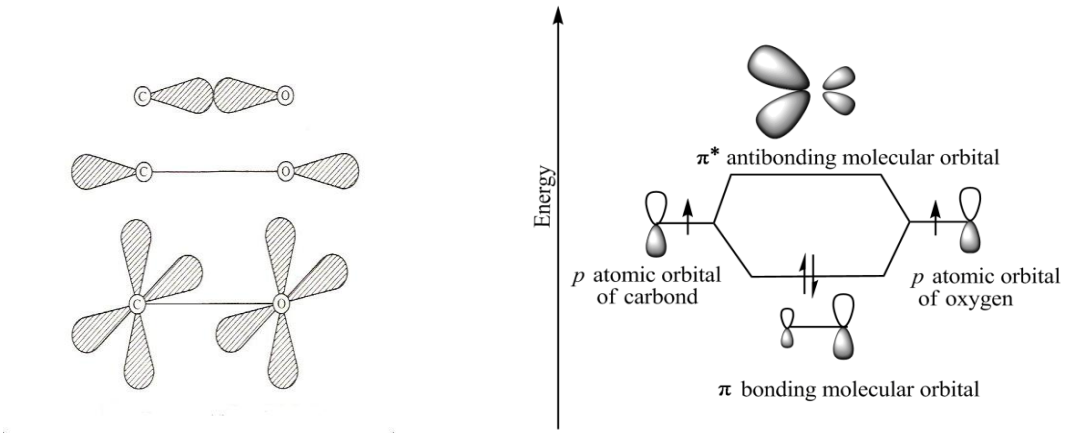

a b

Figure 1.2. (*a*) Bonding in CO molecule[4] (*b*)-A representation of one (of the two) π-bond in CO – the acceptor orbital is the π* combination which has a greater carbon character.

Sketches of the molecular orbitals derived primarily from the 2*p* atomic orbitals of CO shown in Figure 1.3 will give more understanding of its interaction.[4] These sketches include those for N_2 because they are both similar.[4] In spite of the very strong polarity observed in the π bond of CO, the σ and the π overlap populations are very similar to those of N_2.

[4] Miessler, G. L. & Tarr, D. A., *Inorganic Chemistry*, Pearson Education and Pearson Prentice Hall, New Jersey, **2004**.

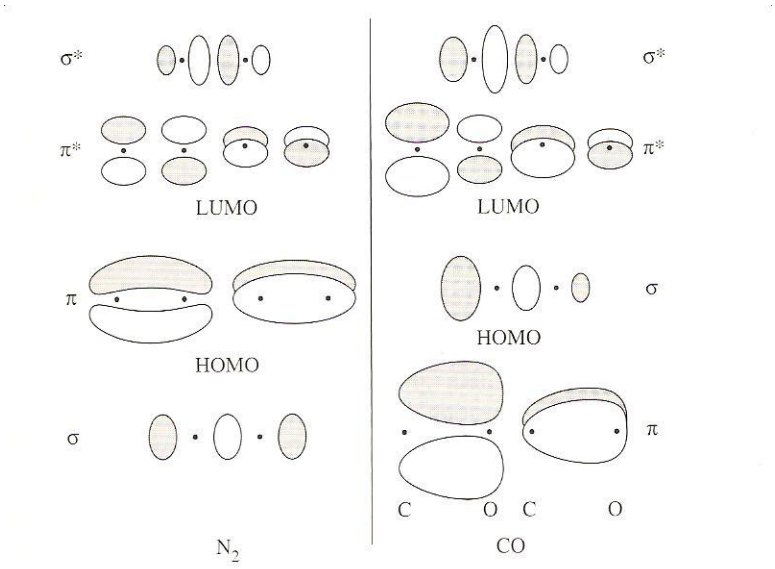

Figure 1.3. selected Molecular Orbitals of N_2 and CO.[4]

Two features of the molecular orbitals of CO deserve attention. First, the highest energy occupied molecular orbital (the HOMO) has its largest lobe on carbon. It is through this orbital, occupied by an electron pair, that CO exerts it σ-donor function, donating electron density directly towards an appropriate metal orbital such as an unfilled *d* or hybrid orbital. Carbon monoxide also has two empty π* orbitals (the lowest occupied molecular orbital or LUMO); these also have larger lobes on the carbon than on the oxygen.[4] This implies that a metal atom having electrons in the d orbital of suitable symmetry can donate electron density to the π* orbitals and this is called the "back bonding". Thus formation of the metal-carbon σ-bond occurs through the overlap of suitable metal d_σ orbitals with sp_σ orbitals on the carbon atom (Figure 1.4). As mentioned above, there is then a metal-to-ligand π-bond formed by overlap of the metal d_π orbitals which should normally contain some electrons with and empty $2p_{\pi^*}$ (antibonding) orbitals on carbon (Figure 1.4).[4] The evidence of this metal-to-ligand or "back" bonding derives from structural data obtained from spectroscopic and electron spin resonance evidences.[3] It is probably this backbonding which stabilizes low oxidation states in carbonyl and nitrosyl complexes. These σ-donor and π-acceptor interactions are both illustrated in Figure 1.5.[3]

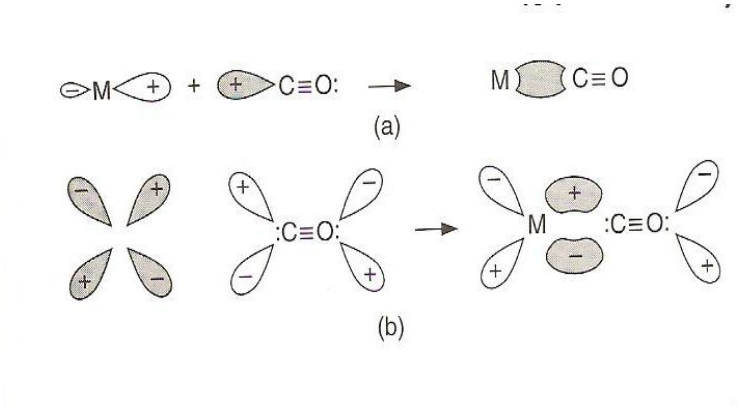

Figure 1.4. (*a*) sigma(σ) bond formed between the metal and the CO ligand. (*b*) Pi (π) bond formed between the metal and the CO ligand.[4]

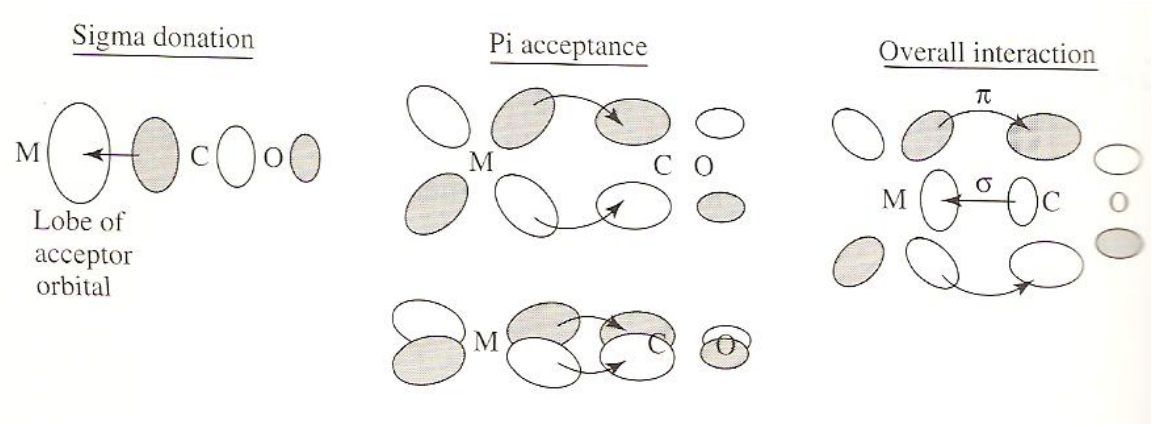

Figure 1.5. σ and π interactions between CO and a metal atom.[3]

These effects when combined together are said to be synergistic (that is the transfer of electron density from metal to ligand renders the σ-donation of the electrons from carbon to the metal easier). This means that CO can donate electron density through its σ orbital to a metal atom and the greater the electron density on the metal, the more effectively it can return electron density to the π* orbitals of CO.[4] The net effect can be strong bonding between the metal and CO.[4] Worth noting is the fact that the strength of this bonding also depends on several factors, including the charge on the complex and the ligand environment of the metal. This as earlier mentioned has been proved by evidence from Infrared spectroscopy and X-ray crystallography. IR spectroscopy (the carbon CO stretching vibration) has also given same results. Results show that the more negative the charge on the organometallic species is, the greater the tendency of the metal to

donate electrons to the π* orbital of CO and the lower the energy of the C-O stretching vibration.[4]

The importance of the catalytic reduction of N_2 to NH_3 has made N_2-bound complexes to be one of the most studied. One of the most common complex known in the study of this process is [HIPTN_3N]Mo(N_2) which has Mo(III) in a low spin (d^3; S=1/2) state.[1] McNaughton L. R. et al[1] in their study proved that this complex could exist in two possible electronic configurations [e^3] and [a^2e^1]. Their calculations proved that the configuration exhibited by this complex is [e^3].[1] Schrock R. R. found out in his work on transition metal complexes that contain a triamidoamine ligand[5] that the d^3 [HIPTN_3N]MoN_2 complex is stable. He also showed that [$C_6F_5N_3$N]ReN_2 has a high stability. Worth noting is the fact that most of these studies have been carried out with the heavier atoms of the transition metals with the most common being Re, Mo and W.

Although dinitrogen (N_2) is isoelectronic with CO and of course isosteric, it is far more inert. As shown above in Figure 1.3, dinitrogen (N_2) has similar molecular orbital arrangement to those of CO. Even though N_2 interacts in the same manner as the CO ligand with a metal atom (Figure 1.6), their π-accepting tendencies are very much different. This is because the N_2 σ* and π* levels are very close together in energy and they are symmetric. On the other hand the corresponding CO levels are farther apart in energy and skewed towards the carbon atom. Due to this fact, N_2 is a weaker ligand than CO. Therefore, the geometric overlap for CO is better and CO has better σ-donor and π-acceptor qualities than N_2. This in turn will account for the poor stability of N_2 complexes in general. This means that the overlap of a transition metal with CO will be totally different in strength from that observed when the transition metal is bound to N_2. This might be one of the reason why complexes with dinitrogen as ligand have often been studied with heavier transition metal complexes due to the presence of more d electrons ready for bonding which with N_2 and the additional protection provided by the triamidoamine ligand pocket.

[5] Schrock, R. R. *Acc. Chem. Res*., **1997,** 30, 9.

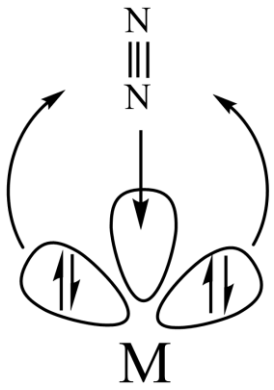

Figure 1.6. Metal-N_2 σ-donor and π-acceptor interactions

1.3 The Triamidoamine Ligand

The structure we are investigating in this work has two ligands bound to it; the CO ligand and the triamidoamine [(**R**$CH_2CH_2N)_3N$] ligand (where **R**= H, CH_3 or C_6H_5). An understanding of the interaction going on in this structure will be more elucidated if we take a close look at all the ligands involved. Previous works done for transition metal complexes with this ligand have often used HITP (**h**exa**i**so**p**ropyl**t**erphenyl) as the auxiliary group because of the way it protects the central metal atom in its "pocket" further binding but in this work I decided to use the auxiliary groups mentioned above so as to ease calculations.

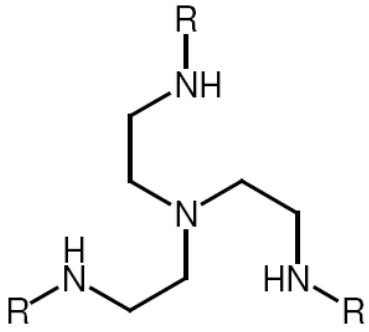

Figure 1.7. The Triamidoamine ligand with R = $SiMe_3$, C_6F_5, or 3,5-(2,4,6-*i*-$Pr_3C_6H_2)_2C_6H_3$ (HIPT = **h**exa**i**so**p**ropyl**t**erphenyl) group.

The bulky triamidoamine ligand ($[(RHNCH_2CH_2)_3N]^{3-}$) is a tetradentate ligand with a -3 charge (Figure 1.7). Three of the terminal nitrogen (the amido nitrogens) bears a -1 charge each while the central nitrogen atom (the amine nitrogen) has no charge and can coordinate with the central metal atom by using it lone pair of electrons. The amido nitrogens are always arranged in a trigonal planar manner so as to maintain the approximate C_3 symmetry of the complex to which it is bound while the amine nitrogen is usually position at the apex of the triamidoamine liagand when bound to the transition metal.

The triamidoamine ligand, generally written as $[(RNCH_2CH_2)_3N]^{3-}$, is a 12-electron donor ligand (4σ, 2π) since one of the three linear combination of the atomic orbitals constructed from the p-orbital on the three amido nitrogens is a ligand centered nonbonding orbital.[6] It can bind to a variety of transition metals especially in the oxidation states of +3 or higher in a tetradentate manner. The best known version currently are those where R = SiMe3 ($[N_3N]^{3-}$) or R =C_6F_5 ($[N_3N_f]^{3-}$) with others like the case where R = HIPT (hexaisopropylterphenyl or 3,5-(2,4,6-*i*-$Pr_3C_6H_2)_2C_6H_3$) are presently under a lot of studies.[7] As mentioned above such ligands usually bind to a metal in a tetradentate manner, thereby creating a sterically protected threefold symmetric "pocket" in which only three orbitals are available to bond to additional ligands in that pocket, two degenerate π orbitals (approximately d_{xz} and d_{yz}) and a σ-orbital (approximately d_{z2}) as shown in Figure 1.8.[5] Some tungsten and molybdenum complexes containing $[N_3N]^{3-}$ or $[N_3N_f]^{3-}$ and HIPT have been synthesized and theoretically extensively studied.[8,9,10]

[6] Schrock, R. R.; Davis, W. M.; Freundlich, J. S. *J. Am. Chem. Soc.*, **1996,** *118*, 3643.
[7] Schrock, R. R. Rosenberger, C.; Seidel, S. W.; Keng-Yu S.; Davis, W. M.; Odom A. L. *J. of Org. Chem.*, **2001**, 617, 495.
[8] Weare W. W.; Hock, A.S.; Schrock, R. R.; Müller,P. *Inorg. Chem.*, **2006**, 45, 9185.
[9] Yandulov, D. V.; Schrock, R. R.; Rheingold, A. L.; Ceccarelli, C.; Davis, W. M. *Inorg. Chem.*, **2003**, *42*, 796.
[10] Mersmann, K.; Hauser, A.; Lehnert, N.; Tuczek, F. *Inorg. Chem.*, **2006**, 45, 5044.

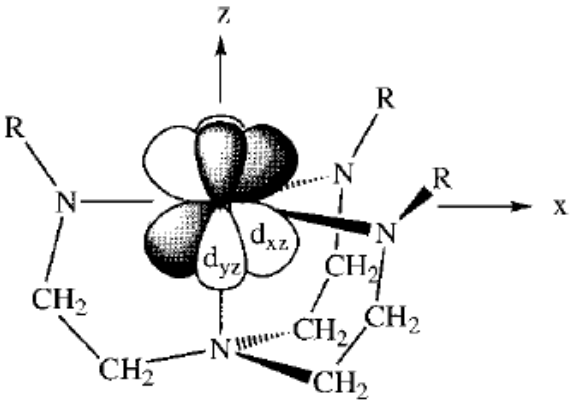

Figure 1.8. Interaction between the metal and the triamidoamine ligand with a display of the various orbitals used.[5]

The fact that the two frontier π orbitals in a C_3 symmetric triamidoamine complex are strictly degenerate and essentially pure d orbitals creates an environment that is especially favorable for formation of a metal-ligand triple bond, but hybrid orbitals can be created readily that allow formation of a metal-ligand double bond plus a metal-ligand single bond or three metal-ligand single bonds.[11] Only two π bonds can form between the metal and the equatorial nitrogen atoms since the linear combination of atomic orbital (LCAO) formed from the nitrogen p orbitals that has an A_2 symmetry in the C_3v point group is a ligand centered nonbonding orbital.[11]

1.4 Why study this complex -$[RCH_2CH_2N]_3NCrCO$ (Where R = H, CH_3, C_6H_5) ?

There are literally thousands of chromium (III) complexes that, with a few exceptions, are hexacoordinate and octahedral. In the case of our complex it is trigonal bipyramidal with apparent C_{3v} symmetry that I later transformed to a Cs symmetry so as to increase the possibilities of varying the Cr-CO restrained bond angle. To understand the bonding in this complex especial between Cr-CO, it will be of great importance to get a good knowledge of the chemistry of the Cr^{3+} (d^3) ion and to understand some properties about it like its electronic structure (whether it is high or low spin) which is of great importance to this work.

[11] Dobbs, D. A.; Schrock, R. R.; Davis, W. M. *lnorg. Chim. Acta,* **1997,** 263, 171.

From an understand of the mode of interaction of the two ligands (triamidoamine and CO) involved here in this research work and the number of electron present in the Cr^{3+} central metal ion that has a d^3 electronic configuration, it is important to note that the complex is low spin with S=1/2 which is not usual for d^3 chromium (III) complexes that are generally known to have three spin-allowed transitions (high spin, S=3/2) with the three electrons occupying three different degenerate orbitals. This unique feature of Cr^{3+} in this complex is the basis for this theoretical study.

CHAPTER 2

BASIC THEORETICAL CONCEPTS

2.1 Ligand Field Theory

Ligand Field Theory (LFT) is a very powerful model to explain trends in geometries, magnetic properties, bond energies, excitation energies, and other physical properties of TM compounds.[12] In particular, the splitting of the d-orbital energy levels in a highly symmetric field of 4-6 ligands is a very helpful model to rationalize molecular properties of TM complexes.[12] LFT can be considered as a simplified MO theory that considers mainly the valence d orbitals of the TM and the frontier orbitals of the ligands. Alternatively, it can also be considered as a more sophisticated version of crystal field theory (CFT), which considers only electrostatic interactions between the metal and the ligands.[12] It treats the metal-ligand interaction as a covalent bonding interaction, and depends upon considering the overlap between the d-orbitals on the metals and the ligand donor orbitals. We can then say that the ligand field theory combines the molecular orbital theory and the crystal field theory. Before we get a pictorial view of the metal d-orbital interaction with the s and p orbitals of a ligand we should take a look at the Crystal Field and Molecular orbital theories.

2.2 Crystal Field Theory (CFT)

Crystal Field Theory is based upon the effect of a perturbation of the d-orbitals consisting of electronic interaction between the metal cation nucleus and the negatively charged electrons of the ligands: the metal-ligand interactions are electrostatic only. CFT successfully accounts for some magnetic properties, colours, hydration enthalpies, and spinel structures of transition metal complexes, but it does not attempt to describe bonding.

The theory is developed by considering energy changes of the five degenerate *d*-orbitals upon being surrounded by an array of point charges consisting of the ligands. As a ligand approaches the metal ion, the electrons from the ligand will be closer to some of the *d*-orbitals and farther

[12] Frenking, G.; Fröhlich, N. *Chem. Rev.*, **2000,** 100, 717.

away from others causing a loss of degeneracy. The electrons in the *d*-orbitals and those in the ligand repel each other due to repulsion between like charges. Thus the d-electrons closer to the ligands will have a higher energy than those further away which results in the *d*-orbitals splitting in energy. This splitting is affected by the following factors:

- The nature of the metal ion.
- The metal's oxidation state. A higher oxidation state leads to a larger splitting.
- The arrangement of the ligands around the metal ion (geometry of complex).
- The nature of the ligands surrounding the metal ion. The stronger the effect of the ligands then the greater the difference between the high and low energy 3d groups.

The most common type of complex is octahedral; here six ligands form an octahedron around the metal ion. In octahedral symmetry the *d*-orbitals split into two sets with an energy difference, Δ_{oct} where the d_{xy}, d_{xz} and d_{yz} orbitals will be lower in energy than the d_{z2} and d_{x2-y2}, which will have higher energy, because the former group are further from the ligands than the latter and therefore experience less repulsions. Tetrahedral complexes are the second most common type; here four ligands form a tetrahedron around the metal ion. In a tetrahedral crystal field splitting the *d*-orbitals again split into two groups, with an energy difference of Δ_{tet} where the lower energy orbitals will be d_{z2} and d_{x2-y2}, and the higher energy orbitals will be d_{xy}, d_{xz} and d_{yz} - the opposite way round to the octahedral case. Furthermore, since the ligand electrons in tetrahedral symmetry are not oriented directly towards the *d*-orbitals, the energy splitting will be lower than in the octahedral case.

Other complex geometries which can be described by CFT are square planar, pyramidal, trigonal pyramidal, trigonal bipyramidal and others. Our greatest concern in this research work will be on the trigonal bipyramidal geometry.

Some of these crystal field splitting models are diagrammatically presented below:

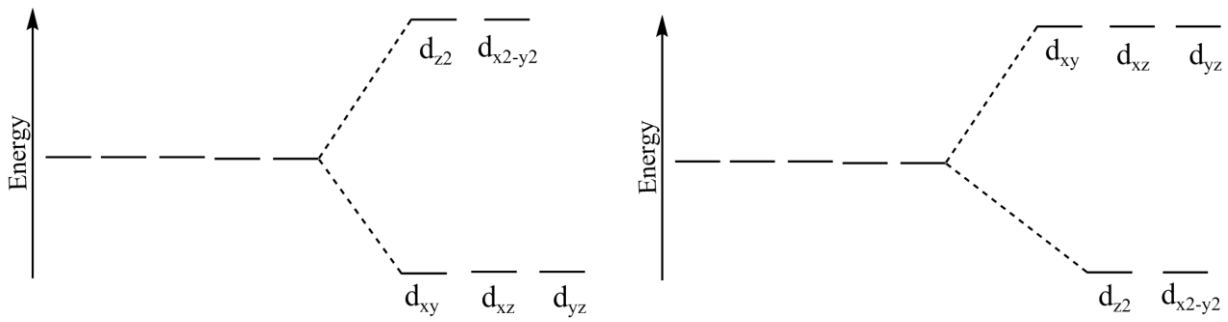

Figure 2.1. Crystal field splitting for a d orbital in a) Octahedral field and b) Tetrahedral field

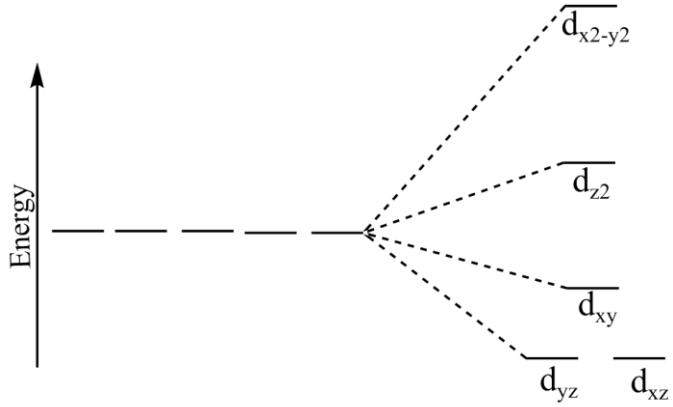

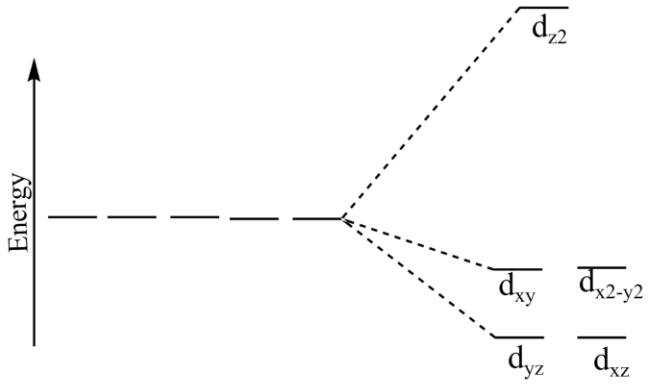

Figure 2.2. Crystal field splitting for a d orbital in A) square planar complex and B) Trigonal bipyramidal complex.

The splitting of the d-orbital degenerate levels in a crystal field is separated for each case by an energy called the Crystal Field Stabilization Energy (CFSE) or for the ligand field theory it is called the ligand field splitting parameter ($\mathbf{\Delta_o}$). This value determines the amount of energy

needed to excite an electron from a lower energy level of a *d* degenerate orbital of a complex with a particular geometry to a higher energy level. When electrons fill these orbitals, the energy levels which become occupied depend on the value of Δ_o. When there are **x** electrons in the t_{2g} orbitals, and y electrons in the e_g orbitals, (for the case of an octahedral complex) the total energy of the electrons relative to the average energy of the electrons is known as the ligand field stabilization energy (LFSE)**.** The LFSE therefore depends on the number of electrons in the d-orbitals of the metal, x+y, the value of Δ_o, and the distribution of electrons between the t_{2g} and e_g levels. As a result we turn to have both high spin and low spin complexes depending on the properties listed above.

Keeping all the other properties constant, we can classify ligands according to the way they influence splitting in the d-orbitals and this gives rise to what is known as the spectrochemical series. The splitting of the *d* orbitals decreases in the following order;

$$CO \approx CN^- > NO_2^- > NH_3 > NCS^- > H_2O > OH^- > F^- > SCN^- \approx Cl^- > Br^-$$

Strong field ligand — weak field ligands

The strong field ligands give rise to a large value Δ_o of and turn to formlow spin complexes while those that give to a small value Δ_o are weak field ligands and turn to form high spin complexes. The strong field ligands are mostly π acceptor ligands.

The splitting of *d* orbitals in the crystal field model not only depends on the geometry of the complex and the ligands that surround the metal, it also depends on the nature of the metal ion, the charge on this ion. When the geometry and the ligands are held constant, this splitting decreases in the following order.

$$Pt^{4+} > Ir^{3+} > Rh^{3+} > Co^{3+} > Cr^{3+} > Fe^{3+} > Fe^{2+} > Co^{2+} > Ni^{2+} > Mn^{2+}$$

Strong field metal ions — Weak field metal ions

Metal ions at one end of this continuum are called *strong-field ions*, because the splitting due to the crystal field is unusually strong. Ions at the other end are known as *weak-field ions*.

2.3 Molecular Orbital (MO) Theory

The MO theory is a method for determining molecular structure in which electrons are not assigned to individual bonds between atoms, but are treated as moving under the influence of the nuclei in the whole molecule. It uses a linear combination of atomic orbitals to form molecular orbitals which cover the whole molecule. These are often divided into bonding orbitals, anti-bonding orbitals, and non-bonding orbitals. If this orbital is of type in which the electron(s) in the orbital have a higher probability of being between nuclei than elsewhere, the orbital will be a bonding orbital, and will tend to hold the nuclei together. If the electrons tend to be present in a molecular orbital in which they spend more time elsewhere than between the nuclei, the orbital will function as an anti-bonding orbital and will actually weaken the bond. Electrons in non-bonding orbitals tend to be in deep orbitals (nearly atomic orbitals) associated almost entirely with one nucleus or the other, and thus they spend equal time between nuclei or not. This picture could be seen in an octahedral complex as shown below.

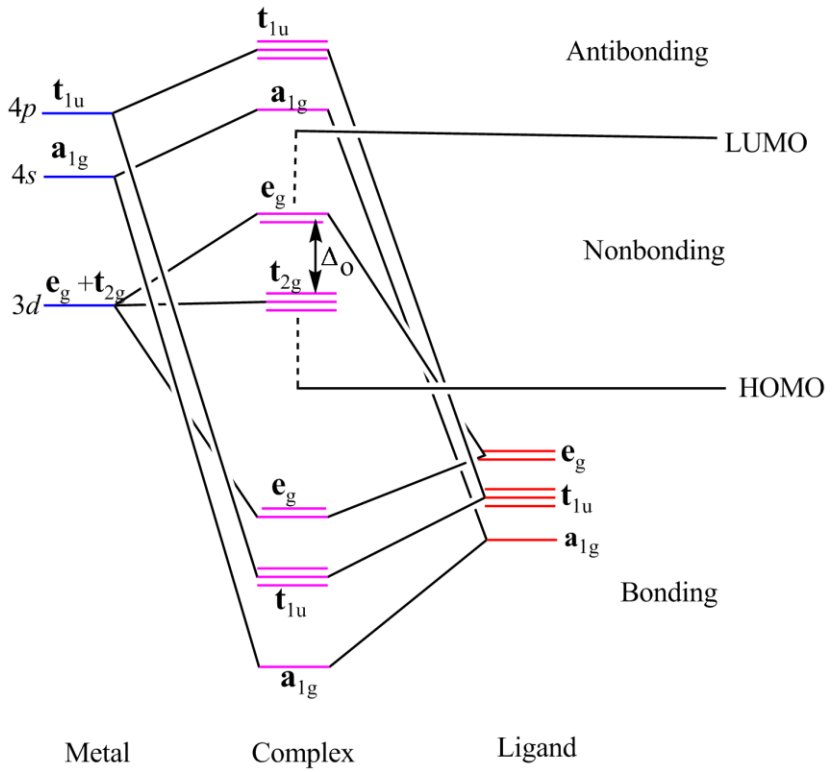

Figure 2.3. Molecular orbital picture of an octahedral complex.

2.4 π-Backbonding

It is of great importance to understand on a general note the bonding that occurs in transition metal carbonyls. This will give us an idea on how the different contributions from the ligand(s) and the metal atom are made for their bonds to be formed and this knowledge might be of great help for us to know the extent to which each of these ligands involved do affect the Cr-CO bond in this complex. One important π bonding in coordination complexes is the metal-to-ligand π bonding, also called π backbonding. This type of bonding often occurs alongside another bonding called the σ-donation which involves movement of electrons from the ligand to the metal (Ligand-to-Metal). Theoretical calculations done on a π-complex of dinitrogen with uranium revealed that there could be a metal to ligand π-backbonding occurring in a molecular species without necessarily having the σ-donation from the ligand.[13]

Backbonding is often observed in metal carbonyls as the predominant interaction that keeps the two species (metal and carbonmonoxide ligand) together. This bonding type has been noted to occur when the LUMOs of the ligand are anti-bonding π^* orbitals. These orbitals are close in energy to the d_{xy}, d_{xz} and d_{yz} orbitals, with which they combine to form bonding orbitals. As you move from left to right on the periodic table, the transition metals show a trend in backbonding tendency due to an increase in the number of electrons available for interaction in the *d* orbital and the absence of an empty *d* orbital. The *d* π backdonation from metals to ligands is always accompanied by a σ-donation from the ligand concerned as mentioned above. According to the increase in *d* electrons, we would expect that as you move from left to right on the periodic table the backdonation tendency increases.

This means that transition metals can interact with ligand through the ligand σ donation to the metal and the metal π backdonation to the ligand, the ligand being a π-acceptor.
carbonmonoxide is not the only π acceptor ligand known. There are others which are; N_2, NO, PR_3, C_2H_4, CN^-, SCN^- , the carbine family (CR_2^-) and many others. Examples of their manner of interaction with a transition metal are seen in the figures below.

[13] Roussel, P.; Errington, W.; Kaltsoyannis, N.; Scott, P. *J. Org. Chem.*, **2001,** 635, 69.

The Dewar, Chatt, and Duncanson (DCD) scheme gives a good explanation for this type of bonding interactions.[14] This scheme explained that for this interaction to occur, there is a σ donation of electron from the ligand to an empty *d* orbital or the metal which has same symmetry as the ligand orbital, which is later followed by a π-backdonation from the metal d_π orbitals to the π* orbital of the ligand which is empty (in the case of PR_3 we have σ* being use in the place of π*).This bonding situation is said to be synergistic; the greater the σ donation to the metal, the greater the pi backbonding. Also, the greater the electron density back-donated into the π* orbital on the ligand, the greater the reduction in the ligand molecular bond order. It has also been proven theoretically that in a metal π-accpetor ligand complex where there is a second π acceptor ligand the backdonation tendency on any of this ligand is affected and this effect is increase depending on the position of the second ligand and the kind of substituent it carries. This has been studied extensively by Gray using X-ray crystallography.[15]

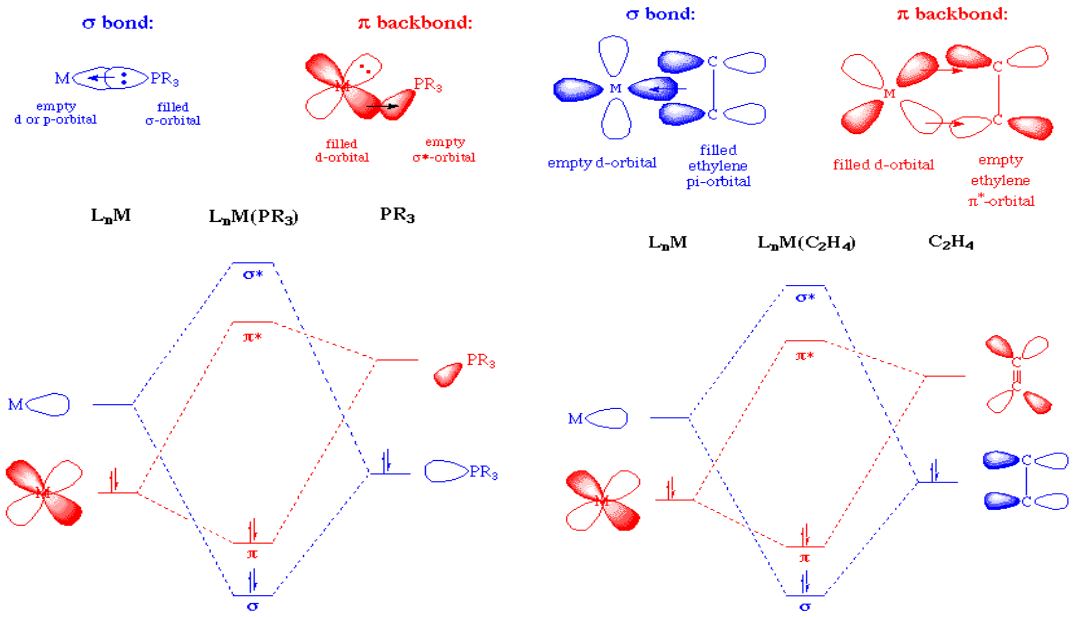

Figure 2.4. (A) ligand π-donation/metal π-backdonation to a σ* orbital in PR_3 (B) ligand π-donation/metal π- backdonation to a π* orbital in a to C_2H_4 ligand.

[14] Bridgeman A. J. *Inorganica Chimica Acta*, **2001,** 321, 27.

[15] Gray, G.M.; Fish, F.P.; Srivastava, D.K.; Varshney, A.; van der Woerd M.J.; and Ealick S.E. *J. Org. Chem.*, **1990,** 385, 49.

2.5 Metal-Carbonyl (CO) Backbonding

There has been a lot of study done on the mode of interaction of the carbon monoxide ligand to transition metal. A detailed understanding of the bonding that exists in CO molecule is required to understand its interaction with transition metals. The bonding in CO is influenced by a couple of thing worth taking note of;

- Zeff(O)>Zeff(C)
- the energy of the O 2s atomic orbital is lower than that of the C 2s atomic orbital.
- the 2p level in O is lower in energy than that in C.
- the 2s-2p separation in O is greater than that in C see Figure 2.5b and 2.6

To generating the orbital interaction diagram for CO we have to assume that only the 2s-2s and 2p-2p atomic orbitals do overlap (Figure 2.5b and 2.6). Two of the most important features to notice here and which are very important for the interaction of the CO ligand with a metal are;

- The highest occupied molecular orbital (MO) called HOMO is σ-bonded and possesses predominantly carbon character; occupation of this MO effectively creates an outward pointing lone pair center on C (see figure 2.5a). It can be noticed that in this CO species, the total overlap population for the π electrons is about twice that for the σ electrons. The most easily ionized electrons of CO are in a molecular orbital such that its gross atomic population is about 94% localized on the carbon atom; these electrons account for the (weak) electron donor properties of CO.
- A degenerate pair of π* (2p) MOs make up the lowest unoccupied MOs (LUMOs); each possesses more C than O character as shown in figure 2.5a. The HOMO and the LUMO orbitals are represented in figure 2.5b.

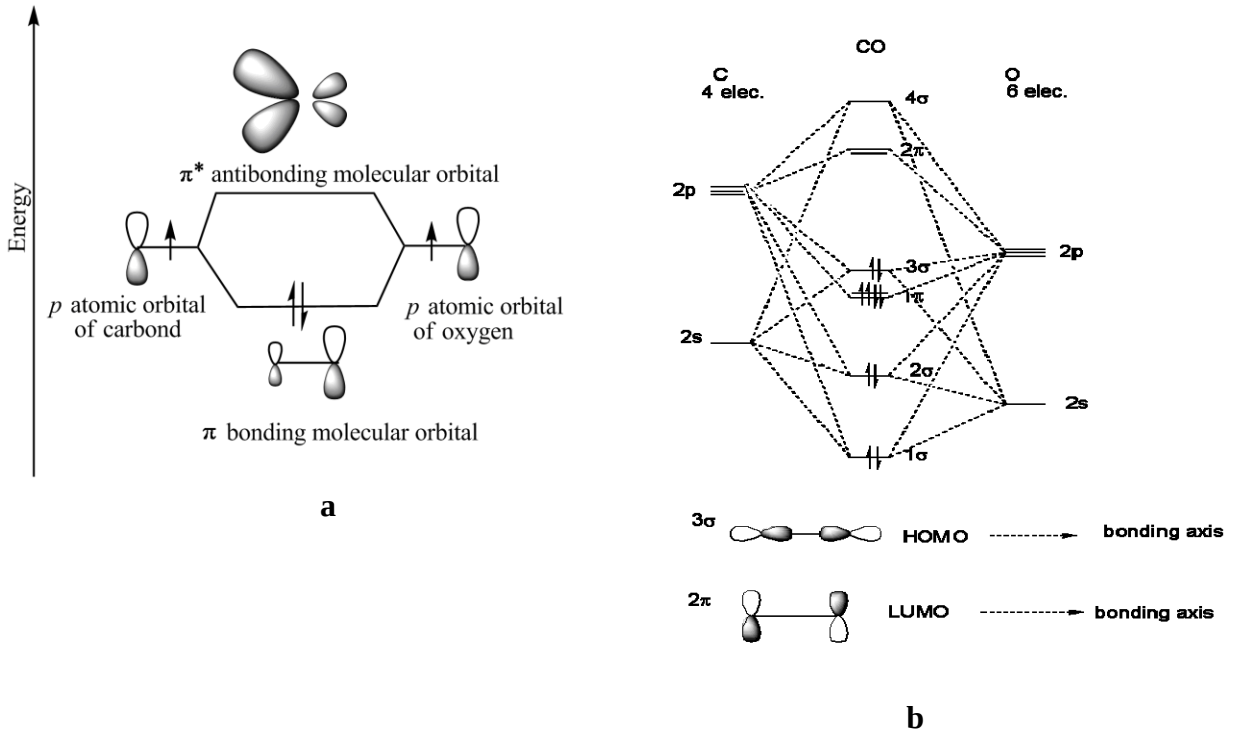

Figure 2.5. (a) Picture showing the large electron density on Carbon for the CO molecular orbital (b) molecular orbital interaction of Carbon and oxygen to form carbon monoxide with the HOMO and LUMO frontier orbitals clearly shown.

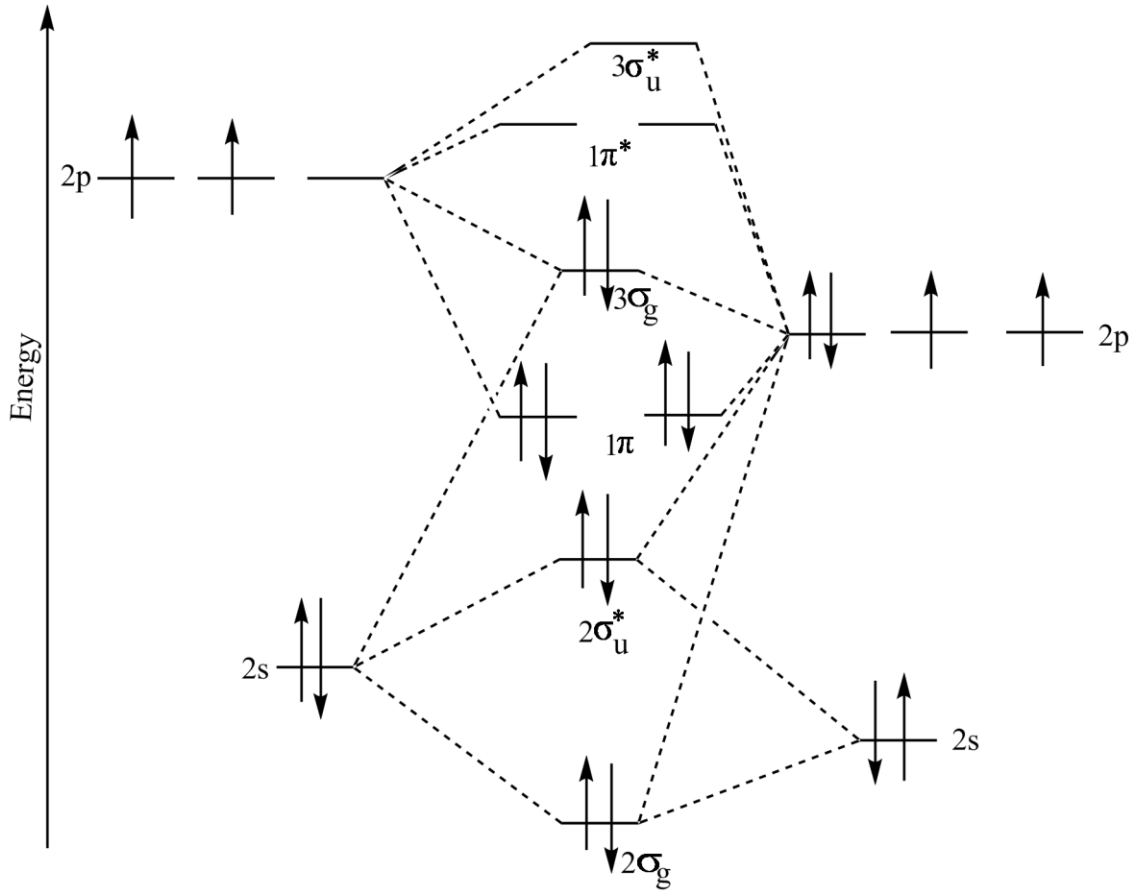

Figure 2.6. The molecular orbital picture of carbon monoxide which clearly shows the true splitting of the mixed carbon and the oxygen molecular orbitals.

Carbon monoxide is a common ligand in transition metal chemistry, in part due to the synergistic nature of its bonding to transition metals. We can describe the bonding of CO to a metal as consisting of two components. The first component is a two electron donation of the lone pair on carbon (coordination exclusively through the oxygen is extremely rare) into a vacant metal *d*-orbital. This electron donation makes the metal more electron rich, and in order to compensate for this increased electron density, a filled metal *d*-orbital may interact with the empty π* orbital on the carbonyl ligand to relieve itself of the added electron density. This second component is called π-backbonding or π-backdonation. This is shown diagrammatically as well as through a simple MO picture below. The MO has been color coded so you can identify each component of the bonding interaction:

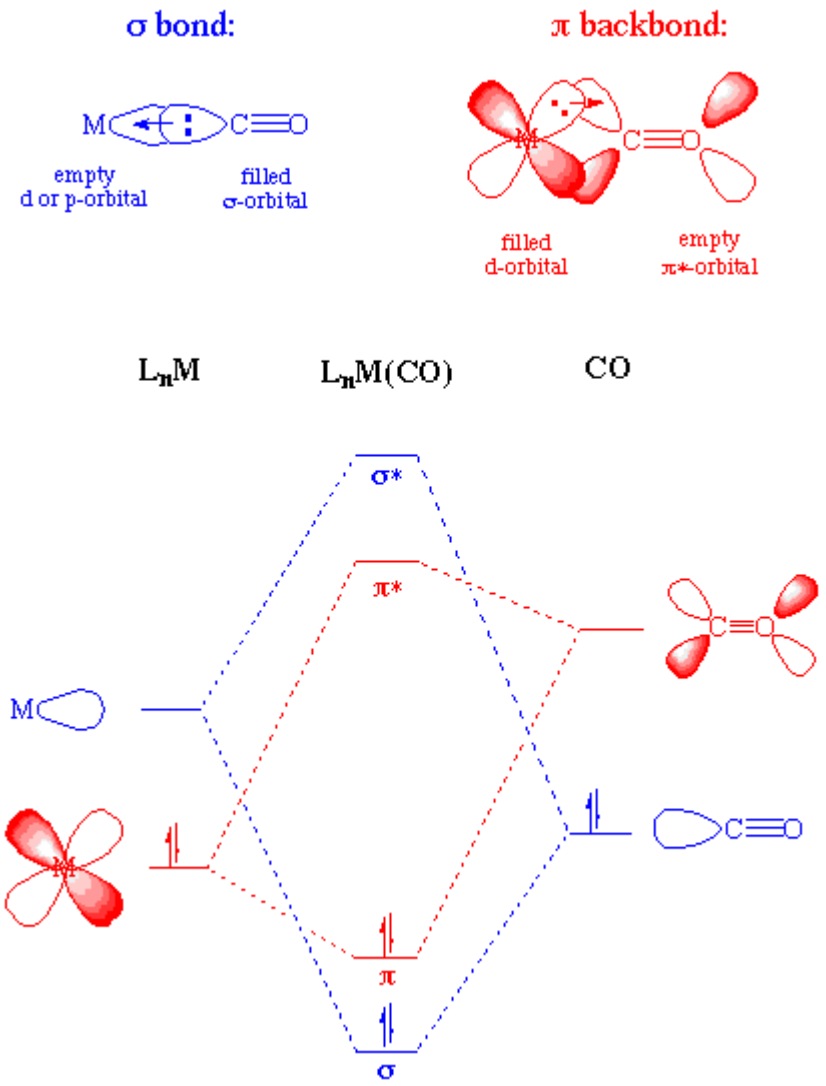

Figure 2.7. Metal-Ligand interaction with the ligand to metal donation and the metal to ligand backdonation shown. The molecular orbital splitting is also shown to explain how the resulting MO for the complex will look like.

The two components of this bonding are synergistic. The more σ-donation by the carbonyl (or other σ-donors on the metal center), the stronger the π-backbonding interaction. Notice that although this involves the occupation of a π* orbital on the CO, it is still a bonding interaction as far as the metal center is concerned. There is a fundamental similarity between the nature of carbonyl-metal bonding and that of alkenes, acetylenes, phosphines, dihydrogen and other π-acceptor ligands.

The occupation of the π* on CO does leads to a decreased bond order in the carbon monoxide molecule itself. As we might expect, as the pi-backdonation becomes stronger, the CO bond

order should decrease from that of the free ligand. Two consequences that we might expect if the CO bond order was reduced would be a lengthening of the C-O bond and a decrease in the carbonyl stretching frequency in the IR. Both of these hold true as seen from the above pictures.

In effect, the DCD model mentioned above, summarily states that the transition metal–carbonyl bond arises from two, mutually enhancing sources:

(i) M←CO σ-donation arises from donation from the slightly antibonding 5σ 'lone pair' function on CO into an empty sd-hybrid on the metal. This mode of bonding tends to strengthen internal bonding in the ligand and hence to increase the CO stretching frequency.[14]

(ii) M→CO π-backdonation results from overlap of filled, or partially filled, d-orbitals of appropriate symmetry on the metal with the low-lying strongly antibonding 2π functions on the ligand. This decreases the internal bonding in the ligand and acts to lower the CO stretching frequency.[14]

These interactions are illustrated in Figure 2.8 (a) which are seen how different they are from main group element counterparts. The model can also be expressed in valence bond theory using resonance hybrids.[14]

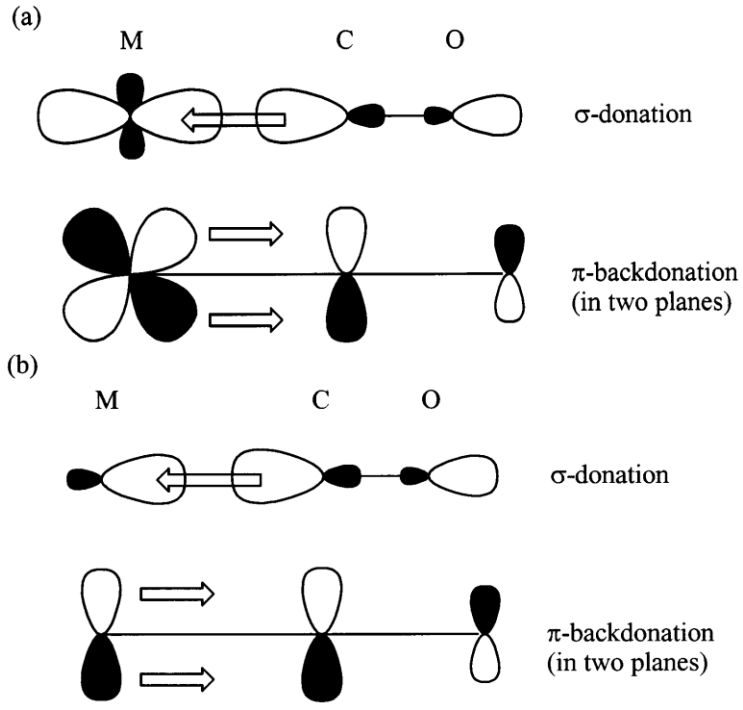

Figure 2.8. Synergic bonding model for (a) transition metal and (b) main group element monocarbonyls.[14]

2.6 A closer look on triamidoamine-supported Cr, Mo, W complexes.

A) Bonding

The chemistry of the group 6 triamidoamine complexes have been extensively studied especially those for the heavier elements (Mo and W). Researchers have tried to understand the bonding in these complexes and to what extend that it does influence their catalytic activities. Theoretical calculations have been employed to get a good picture of these interactions and some of the compounds have been experimentally prepared. The study of these complexes has been divided into two groups; the trigonal monopyramidal (complexes with no axial ligand at top apical position) and the triganoal bipyramidal (complexes with an axial ligand at the apical position) groups.[5] Amongst the group 6 metals, the Mo and W triamidoamine complexes have been widely studied and known but the related Cr compound are very rare. This is the more reason why I decided to work on the carbonyl complex of chromium (III) triamidoamine. The triamidoamine ligand has been often used with substituent HIPT=3,5-(2,4,6-i-$Pr_3C_6H_2)_2C_6H_3$ (hexaisopropylterphenyl) to prevent any bimetallic reactions (because it give a stable and an unreactive bimetallic species) since it maximizes steric protection of a metal coordination site in a monometallic species.[16] Worth noting is the fact that more research emphasis is placed on the trigonal bipyramidal species because they are catalytically more active than the trigonal monopyramidal species.[17]

As mentions in chapter 1, the triamidoamine ligand is trianionic and binds to an early transition metal in a relatively high oxidation state (+3 or higher) in a tetradentate fashion, leaving three orbitals for binding substrates in the trigonally symmetric "Pocket" surrounded by the three amido substituents or the auxiliary groups. Two of these orbitals have π symmetry (that is d_{xz} and d_{yz}) and one has sigma symmetry (d_{z2}). These orbitals can be employed in three combinations ($2\pi/1\sigma$, $1\pi/2\sigma$, or 3σ) to bind substrates in the trigonal pocket. Distortion of the pseudotrigonal symmetry to yield pseudo-octahedral species, or even seven-coordinate species, is possible in

[16] Weare W. W.; Dai X.; Byrnes, M. J.; Chin, M. J.; Schrock, R. R.; Müller,P. *PNAS*, **2006**, 103, 17099.
[17] Weare W. W.; Hock, A.S.; Schrock, R. R.; Müller,P. *Inorg. Chem*., **2006**, 45, 9185.

cases where tungsten (W) is the central metal and strongly bound substrates such as isocyanides or acetylenes are involved.[17] Due to the fact that the d_{xz}, d_{yz} (involved with π bonding) and d_{z2} (involved with σ bonding) orbitals of the central metal atom can be employed in three combinations, these complexes are thus able to bind with ligands at the top apical positions in different modes forming single bonds, double bonds or triple bonds and this could be a head on binding or a side on binding (figures with examples). In complexes that contain the triamidoamine ($[(RNCH_2CH_2)_3N]^{3-}$) ligand only two Metal-Equatorial Nitrogen(Neq) π-bond can be formed in which case the ligand donates 12 electrons to the metal center. However, orbital overlap is more favorable for one of the two π-bonds, so in most cases essentially only one M-Neq is present and the $[(RNCH_2CH_2)_3N]^{3-}$ ligand can be said to contribute only 10 electrons to the total electron count.[5,18] Schrock *et al* prepared the d^2 Chloride triamidoamine complexes of Mo and W ($[N_3N]MCl$,M = Mo or W) and they discovered by theoretically calculations that the $[N_3N]MCl$ complexes are paramagnetic presumably as a consequence of the two electrons being in the degenerate d_{xz} and d_{yz} orbitals.[5]

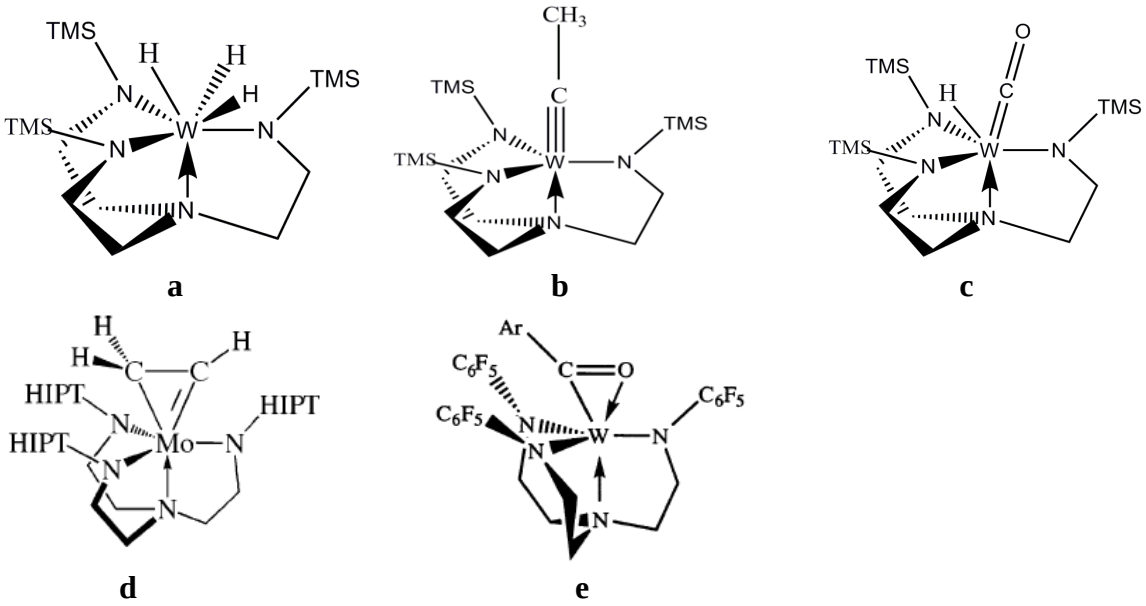

Figure 2.9. (a) 3 σ-bonded W complex.[11] (b) a 2π/1σ (triply) bonded W complex.[11] (c) 1π/2σ bonded W complex.[11] (d) A side on 1π/2σ bonded Mo.[19] (e) a side on 1σ/1σ (kind of dative coordination) bonded W complex.[7]

[18] Schrock, R. R.; Greco, G. E. *Inorg. Chem.*, **2001,** 40, 3850.

[19] Byrnes, M. J.; Dai X.; Schrock, R. R.; Hock, A.S.; Müller,P. *Organometallics*, **2005,** 24, 4437.

B) Bonding in Chromium complexes stabilized by the Triamidoamine Ligand

Theoretical Calculations using Evans method where carried out on chromium (IV) triamidoamine complex [Cr(N_3N)Cl] (**1**; $(N_3N)^{3-}$) (($SiMe_3NCH_2CH_2)_3N)^{3-}$), chromium (IV) alkyls [Cr(N_3N)R] (**2**, R = Me; **3**, R = n-Bu),[20] and on [Cr(N_3N)] (**4**) [21] which revealed the magnetic moments of these complexes at 24^oC and 23 ^oC as 2.9 μ_B (**2**) and 2.8 μ_B (**3**) [which are close to the expected spin-only value (2.83 μ_B) for two unpaired electrons],[20] 3.8μ_B (**4**) and 2.7μ_B (**1**)[21] (which are close to the spin-only μ_{eff} values expected for a high-spin d^3 and d^2 metal complex, respectively). it was then found out that for the case of **2** and **3**, the values agrees with the results of DFT calculations, which show that the d orbital of the complex [Cr(N_3N)H] adopts a triplet ground state configuration with the two unpaired electron occupying two almost degenerate, metal-based d orbitals of π-symmetry (d_{xz} and d_{yz}, if the Cr-R bond is taken as the z axis of the Cartesian coordinate system).[20] The molecular structure of **1** and **4** where determine by single-crystal X-ray diffraction studies and they revealed a trigonal monopyramidal coordination geometry for complex **4** and trigonal bipyramidal coordination geometry for complex **1**.[21] These calculation went on further to reveal that the Cr-N_{amine} bond was longer for **4** than for **1** which was explained by a simplified frontier orbital scheme that the bonding involves two degenerate metal-centered pi-orbitals (approximately d_{xz} and d_{yz}) at lower energy and one σ-orbital (approximately d_{z2}) at slightly higher energy where all there are occupied with one electron in **4**.[21] Due to the anti-bonding contribution of the d_{z2} orbital to the Cr-N_{amine} bond, occupation of this orbital with one electron should cause an elongation of the Cr-N_{amine} bond.[21]
Filippou *et al*,[22,23] reported for the complex [Cr(N_3N)X] (where X= F, Cl, Br, I, CN and H while N_3N= $Me_3SiNCH_2CH_2)_3N$), there is a conformational distortion of the central Cr atom from the equatorial plane defined by N1, N2 and N3 amido nitrogens on the triamidoamine ligand for the cases with X= Br, CN and H. They suggested that all the structural features indicate an extensive π-electron donation of the N_3N ligand to the central metal atom.

---

[20] Filippou, A. C.; Schneider, S. *Organometallics*, **2003,** 22, 3010.
[21] Schneider, S.; Filippou, A. C. *Inorg. Chem.*, **2001,** 40, 4674.
[22] Filippou, A. C.; Schneider, S.; Ziemer B. *Eur. J. Inorg. Chem.*, **2002**, 2928.
[23] Filippou, A. C.; Schneider, S.; Schnakenburg G. *Angew. Chem. Int. Ed*., **2003**, 42, 4486.

Though very little work has been done on chromium complexes bearing a triamidoamine ligand as compared to its Mo and W counterparts, it has been observed that these complexes do follow the same bonding scheme for the Metal-Ligand interaction as presented by the DCD model.

2.7 Molecular Orbital Theory as applied to transition metal complexes with trigonal bipyramidal geometry.

One of my main interests in this research work is the trigonal bipyramidal geometry of the triamidoamine complex with C_3v symmetry (that is later given Cs symmetry) that I have worked on. It is necessary to get a general picture of the way compounds with this structure appear in the ligand field theory (which combines both the crystal field and molecular orbital theories) since I will have to be using this idea to explain the bonding that occurs in these complexes. In the trigonally bipyramidal transition metal triamidoamine complex with C_3v and Cs symmetries, the possible overlaps can only occur with orbitals that are having the same symmetries. It is important to note that the trigonal bipyramidal geometry is one of the only cases where bond angles surrounding an atom are not identical which is simply because there is no geometrical arrangement which can result in five equally sized bond angles in three dimensions. The table below gives us an idea of the symmetry of the various orbitals that might possibly overlap.

Table 2.1. Correlation of the C_3v and Cs irreducible representations with the orbitals involved in interaction. The ligand considered in this case is CO.

Orbital			Point Group	
			C_{3v}	C_s
Metal Orbitals	d_{xy}		e	a'
	d_{xz}		e	a"
	d_{yz}		e	a"
	d_{z2}		a^1	a'
	d_{x2-y2}		e	a'
Ligand Orbitals	HOMOs	$3\sigma_g$	a^1	a"
	LUMOs	$1\pi^*$	e	a'
		$1\pi^*$	e	a'

The orbitals that will overlap will depend on the type of axial ligand we have. McNaughton et al[1] in their study of the EPR study of the low–spin [d^3; S=1/2], Jahn-Teller-Active, dinitrogen

complex of a Molybdenum triamidoamine ([HIPTN$_3$N]MoN$_2$) showed that [HIPTN$_3$N]MoN$_2$ with the ground state of ^{2}E might have two possible electronic configuration; [e^3] and [a^{2}e^1] if there is a Jahn-Teller distortiong.[1]Their work concluded that the [e^3] thus exist.[1] This tells us that these complexes could have different kinds of overlap. The figure below which show the splitting of the d^3 complex at the doubly degenerate ground state (^{2}E) gives us an idea of some of the possible *d*-orbital spitting and hence overlaps that could possibly arise in these complexes.

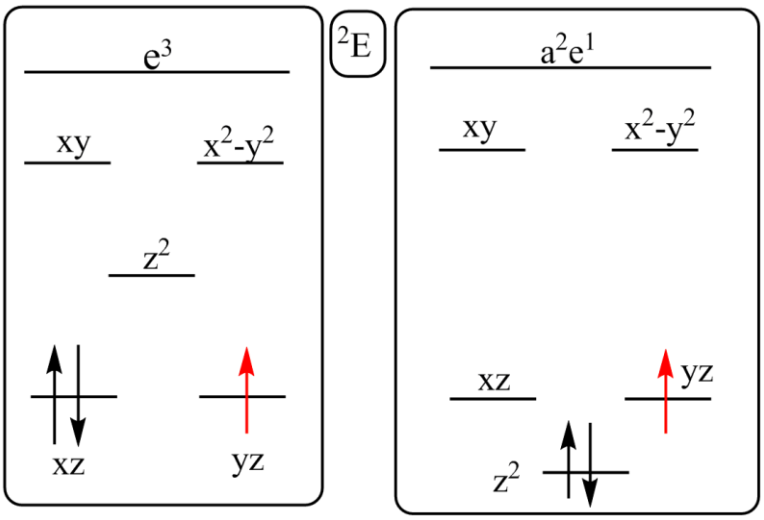

Figure 2.10. Ground state of [HIPTN$_3$N]MoN$_2$ with two possible splitting [e^3] and [a^{2}e^1] where the [e^3] was discovered to be the possible splitting for this complex.[1]

CHAPTER 3

METHOD

What is needed is a good strategy that allows us to understand the underlying principles that causes the Cr-CO bond to have a weaker backbonding and the extent of the ligand donation which will further explain and proof the fact that the complex is peculiar.

The theoretical calculations done in this research work on the bonding in triamidoamine-supported chromium III carbonyl complex with a submaximal backbonding was carried out using the Amsterdam density function (ADF) software package which runs on the snowstorm super computer in the university of Tromsø, Norway. The density function theory is suitable for this research work because it gives superior accuracy to hartree-fock theory and semi-empirical approaches. Also, it is well suited for molecules containing metal atoms. In contrast to the conventional ab initio methods (MP2, Cl, CC), it enables accurate treatment of systems with several hundred of atoms (or several thousand with QM/MM).[24]

The research is strategically divided into six parts;

1) A DFT/OLYP geometry optimization of $[(C_6H_5N)_3N]CrCO$ using the C_3v, Cs and the C_1 point groups. The C_3v and the C_1 point group calculations were done so as to confirm that the Cs calculations were properly done.

2) A DFT/OLYP geometry optimization of $[(C6H_5CH_2CH_2N)_3N]CrCO$ using their irreducible representations (occupation specified in this case) in single-group symmetry. These calculations were done for the C_3v, Cs and the C_1 point groups for the same reason mentioned above. Then, a further calculation was done for another occupation in which case the beta electron of the lower orbital of the complex was promoted to a higher orbital. This was done so as to work with the structure in an excited state and in a ground state (default occupation obtained from the ADF program).

[24] Baerends, E.J *et al*, **ADF2006.01**, SCM, *Theoretical Chemistry*, Vrije Universiteit, Amsterdam, The Netherlands

3) A DFT/OLYP geometry optimization of $[(C6H_5CH_2CH_2N)_3N]CrCO$ using fixed or restrained Cr-CO bond angles; 140^o, 150^o, 160^o, 170^o, 180^o, for the Cs point and plotting them against their restive total bonding energies.

4) Step 2 and 3 were repeated for the complex with hydrogen (H), and methyl (CH_3) as auxiliary groups replacing the C_6H_5 group in the complex $[(C6H_5CH_2CH_2N)_3N]CrCO$. This implies that a DFT/OLYP calculation combining step 2 and 3 was done on the complexes $[(HCH_2CH_2N)_3N]CrCO$ and $[(CH_3CH_2CH_2N)_3N]CrCO$. This was done so as to see how the auxiliary group affects the complex electronically and structurally.

5) Furthermore, a DFT computation was carried out with different exchange Functionals (OPBE, BLYP, and PW91) repeating step 2 and 3 so as to confirm the results obtained with the DFT/OLYP computations.

6) Finally, orbital plots were obtained using the ADF densf analysis program to give a pictorial view of the orbitals involved and the extent to which they bond in the complexes $[(HCH_2CH_2N)_3N]CrCO$, $[(CH_3CH_2CH_2N)_3N]CrCO$, $[(C6H_5CH_2CH_2N)_3N]CrCO$ from the DFT/OLYP results.

For all my calculation done in this work, I have used the ADF program system with the underlying theory being the Kohn-Sham approach to the Density-Functional Theory (DFT). Kohn-Sham DFT is an important first-principles computational method to predict chemical properties accurately and to analyze and interpret these in convenient and simple chemical terms.[24] I most of the calculation I did, I used the OLYP exchange correlation functional which combines the Handy's OPTX modification of Becke's exchange functional (O) and the correlation functional of Lee, Yang, and Parr which includes both local and non-local terms (LYP).[24] I also did use the DFT functionals OPBE (which combines the Handy's OPTX modification of Becke's exchange functional (O) and the 1996 functional of Perdew, Burke and Ernzerhof), BLYP (which combines Becke exchange functional B and the LYP correlation functional), PW91 (the Perdew and Wang's 1991 gradient-corrected correlation functional), BP86 (which combines the Becke's 1988 functional B, which includes the Slater exchange along with corrections involving the gradient of the density and the gradient corrections of Perdew, along with his 1981 local correlation functional P86) to confirm my results.[24]

The Slater type valence triple zeta plus 2 polarization function (TZ2P) basis set was used throughout all the calculations I did because it has an average error that is clearly below 1kcal/mol (the famous chemical accuracy) and it gives a fine mesh for numerical integrations for geometry optimizations with appropriate symmetry constraints and tight criteria as implemented in the ADF program system.[24] The geometry optimization done was carried out with tighter convergence criteria than the default given by the ADF program package.

Open-shell molecules (the system has unpaired electrons) were studied with spin-unrestricted calculations in general. Calculations were done with different substituents on the triamidoamine amido nitrogens to see the influence of side groups on the bonding between Cr and C. The following molecules where studied in each case the spin occupation was varied for the d orbitals of the metal so as to obtain results for one excited state.

$[C_6H_5NCH_2CH_2]_3NCr^{III}CO$ (Cs, S=1/2)

$[CH_3NCH_2CH_2]_3Cr^{III}CO$ (C_s, S=1/2)

$[HNCH_2CH_2]_3NCr^{III}CO$ (C_s, S=1/2)

One of the few negative aspects of using the DFT method which is worth mentioning is that there is always an uncertainty about which method may work best for a given system.[25] To overcome this negative aspect, all the results obtained for the DFT/OLYP method used were further confirmed by the use of other functional. Research has shown that the LYP methods usually over estimate the metal-CO bond length. I have tried to also reduce the error margin that might be obtained from this over estimation of bond length by using tighter criteria for all my calculations.

[25] Sniatynsky, R.; Cedeño D. L. *J. Mol. Structure (Theochem)*, **2004**, 711, 123.

CHAPTER 4

RESULTS AND DISCUSSION

4.1 Observed trends with Restrained Cr-C-O bond angle

In this thesis I have taken a closer look at the geometric and the electronic structure of the triamidoamine-supported Cr(III) carbonyl complex with the results obtained from the DFT calculations done to understand the interaction that is going on around the Cr III central ion and specifically to get a better insight on its interaction with the CO axial ligand. Different trends for the total bonding energy of the species studied were observed. The core of the triamidoamine ligand in all the complexes optimized stayed as C_3 symmetry. For all calculations, only one parameter is varied at a time so as to clearly observe the changes in the molecular geometry and electronic structure of the complexes.

A) Computation with Restrained Angles

Restraining the Cr-C-O bond angle for each of the complex to 140^o, 150^o, 160^o, 170^o, and 180^o and performing a geometry optimization with the DFT/OLYP XC-functional gave interesting trends for the total bonding energies (TBE). These calculations were only possible with the Cs point group because for the C_3v point group, restraining the angle to anything other than 180^o destroys the symmetry hence defeating the purpose of using the point. That is why I decided to transform the point group of all structures used in these calculations to Cs.

The observed trends for results of the complex $[C_6H_5NCH_2CH_2]_3NCr^{III}CO$ (**1**) presented in the relative energy plot shown in Figure 4.1 revealed that the structural conformation with Cr-C-O restrained bond angle of 140^o has the highest total bonding energy of -8221.85Kcal/mol while that with 180^o has the least total bonding energy of -8236.06Kcal/mol. This could be attributed to the fact that the structural conformation of **1** with the Cr-C-O restrained bond angle of 180^o has the most stable geometric arrangement for this complex. This stability is confirmed by the picture presented in Figure 4.2 with complete interaction occurring for the HOMO of the

conformation as compared to others. To this effect, I had to use this conformation for most of the general analysis.

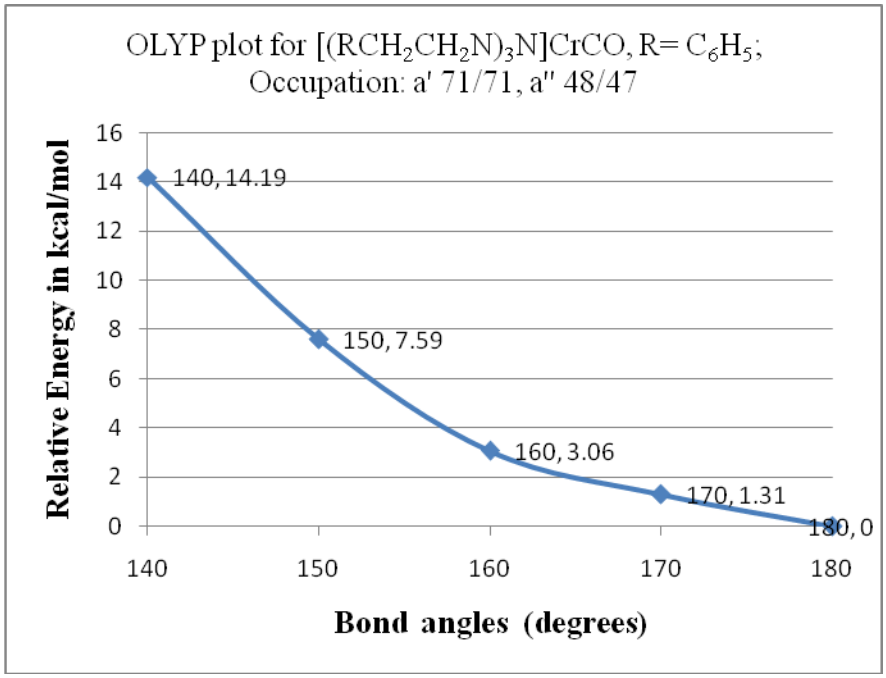

Figure 4.1. Curve showing decrease in relative energy for $[C_6H_5NCH_2CH_2]_3NCr^{III}CO$ possibly imply that the Cr-CO bond of this complex is linear or approximates linearity.

B) Computations with Occupational Considerations

For a qualitative understanding of the electronic structure of this transition metal complex and its orbitals involved in bonding with the ligand, occupation number calculations represent a very valuable tool. After performing another computation with the same parameter mentioned above and moving a spin occupation from a lower orbital to a higher one of the complex $[C_6H_5NCH_2CH_2]_3NCr^{III}CO$ the same trends were observed (decrease in TBE as restrained angle increases) but for the fact that for each of the restrained bond angles of Cr-C-O a slight difference in values for total bonding energies were obtained for the two occupations as shown in Figure 4.3 and 4.1. This increase in total bonding energies is as expected because a single spin has been moved from a lower orbital to a higher orbital consequently increasing the respective bonding energies.

Looking at the energies of these orbitals involved, we will have a good picture of what is actually going on. The spin was move from a' 71 (d_{z2}) orbital with an energy value of -3.340E (eV) to a" 48 (d_{yz}) orbital with an energy value of -2.914E (eV) which can be seen to be higher in energy than the previous orbital (these values are obtained before the spin is moved). After the spin has been moved the reverse happens were orbital a' 71 becomes unoccupied with higher energy of -2.947E (eV) while a" 48 becomes occupied with energy -3.299E (eV). Comparing the two cases for the occupied (HOMO) and the unoccupied orbitals, we would realize that the second case has an occupied orbital of slightly higher energy than the first. Figure 5.2 gives us additional information concerning the type of orbital directly involved in π-back bonding between the metal to ligand in the system. Figure 4.2 depicts that as the Cr-C-O restrained angle increases, there is an overlap increases for both cases hence the difference in the energies of their occupied orbitals is felt more by the complex which directly results in as increase in the difference of their total bonding energies. This directly results in a decrease in the Cr-C1 bond length as the restrained angles increases as can be seen in Table 4.2 B. The difference in TBE is clearly seen when we compare the values shown in Figure 4.3 with those of Figure 4.1.

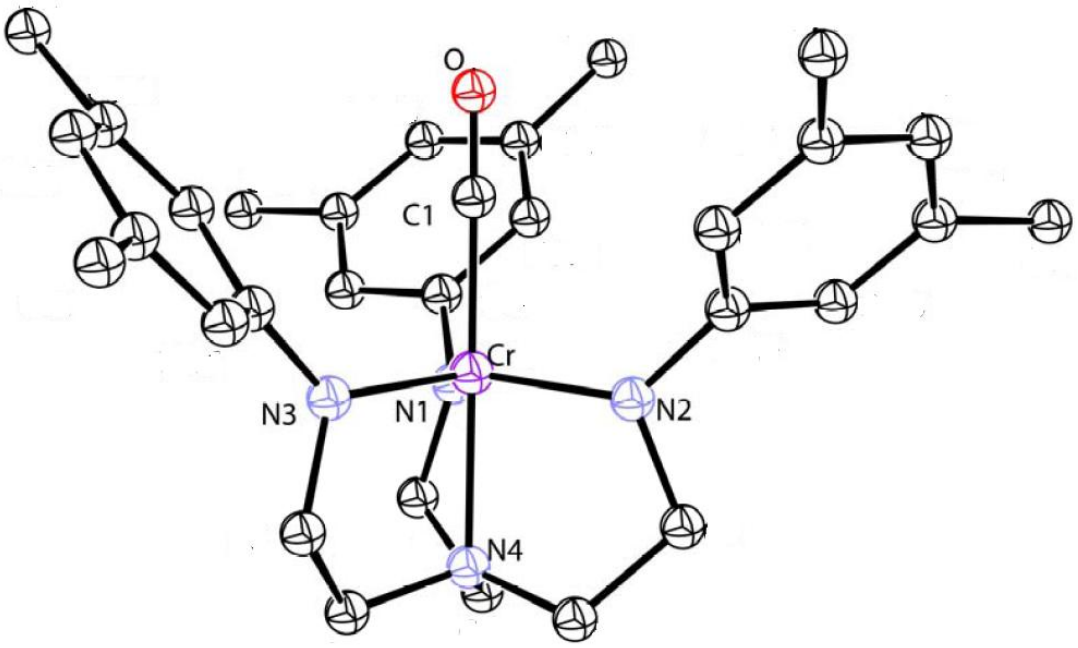

A

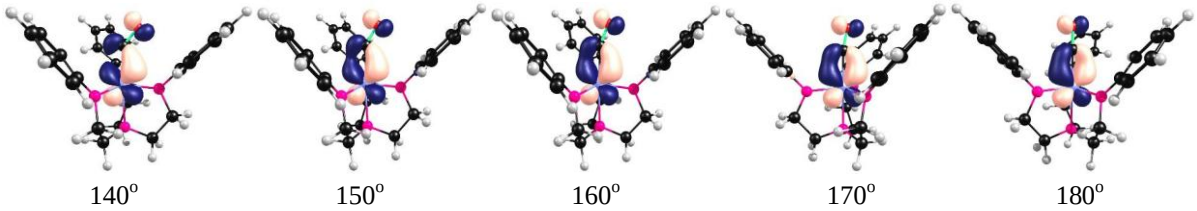

140° 150° 160° 170° 180°

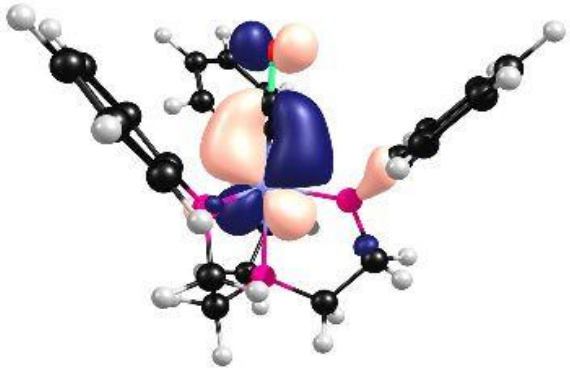

HOMO for occupation 1 using the conformation with Cr-C1-O restrained angles of 180°

Scheme 1

140° 150° 160° 170° 180°

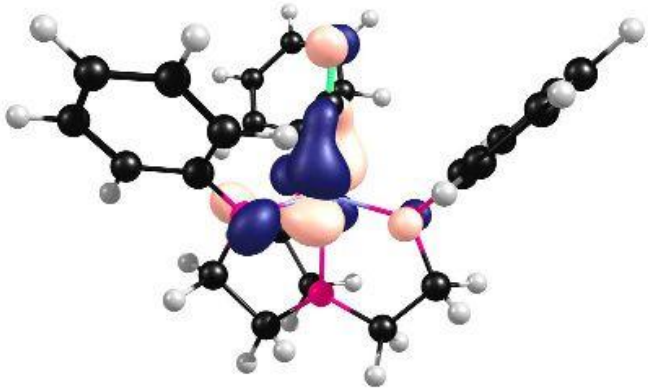

HOMO for the complex with occupation 2 using the conformation with Cr-C1-O restrained angles of 180°

Scheme 2

B

Figure 4.2. (A) Labeled $[C_6H_5NCH_2CH_2]_3NCr^{III}CO$ complex with which all bond lengths and angles used tables below can be visualized as the values are being looked up. (B) **Scheme 1**-orbital overlap increase for d_{xz} orbital (a'71) of metal with liagnd as the Cr-C1-O angle increases. HOMO picture shows that metal d_{xz} – ligand interaction is predominant here. **Scheme 2**-orbital overlap increase for d_{yz} orbital (a"48) of metal with liagnd as the Cr-C1-O angle increases. HOMO picture shows that metal d_{yz} – ligand interaction is predominant here.

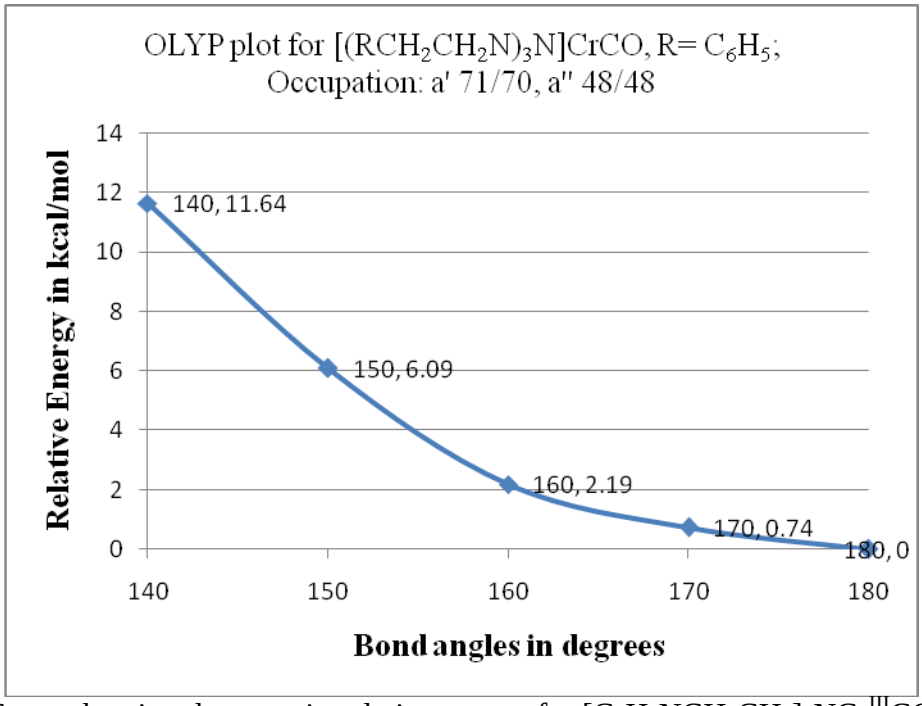

Figure 4.3. Curve showing decrease in relative energy for $[C_6H_5NCH_2CH_2]_3NCr^{III}CO$ with reversed spin Occupation

Geometry optimization of the above complex with only the substituents on the triamidoamine amido nitrogen (auxiliary groups) being varied where the substituents used are Hydrogen and the methyl group alongside the phenyl group, gave the same trend as reported above for the TBE which decrease as restrained angle increases. It was also observed that their different occupations had a difference in the total bonding energies. Notwithstanding, the values for the total bonding energies were much higher for the case of hydrogen (H) and methyl groups (CH_3). The Figure 4.4 below gives a clear picture of these trends which were observed.

When other XC functionals were used, the same results were observed for the $[C_6H_5NCH_2CH_2]_3NCr^{III}CO$ complex by varying the Cr-C-O restrained angles but these values were very much different and had very little agreements (see table below). The trends shown in Table 4.1 can also be seen graphically for some of these funtionals as presented in Figure 4.5 below.

Table 4.1. Showing trends in Relative energy in kcal/mol for different functionals.

Bond angles (deg)	Relative energy in kcal/mol for different functionals					
	Occupation: a' 71/71, a" 48/47			Occupation: a' 71/70 and a" 48/48		
	OLYP	BLYP	PW91	OLYP	BLYP	PW91
180	0	0	0	3.36	2.68	2.76
170	1.31	1.29	1.43	4.1		3.49
160	3.06	2.64	2.64	5.55	5.1	5.21
150	7.59	6.75	6.93	9.45	8.69	8.93
140	14.19	12.83	13.38	15	13.85	14.3

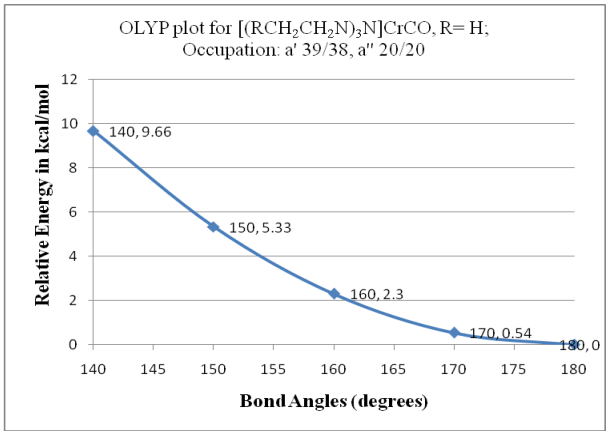

A

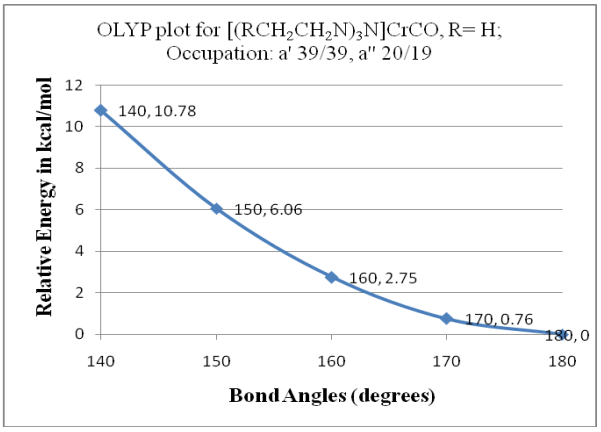

B

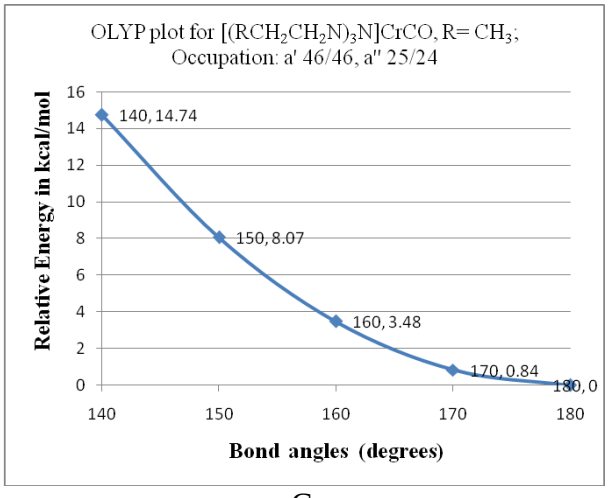

C

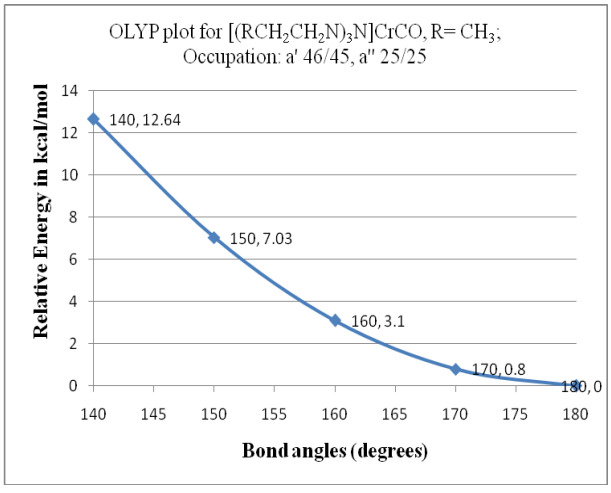

D

Figure 4.4. Relative energy in kcal/mol vs restrained bond angles for different substituents on the amido nitrogen of triamidoamine with their respective reverse spin occupation plots.

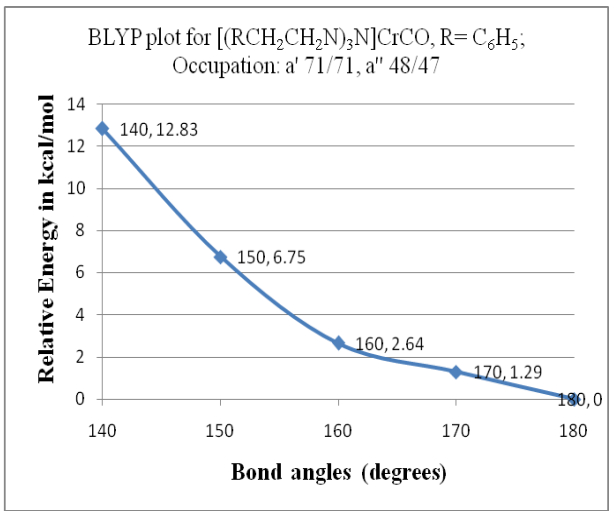

A

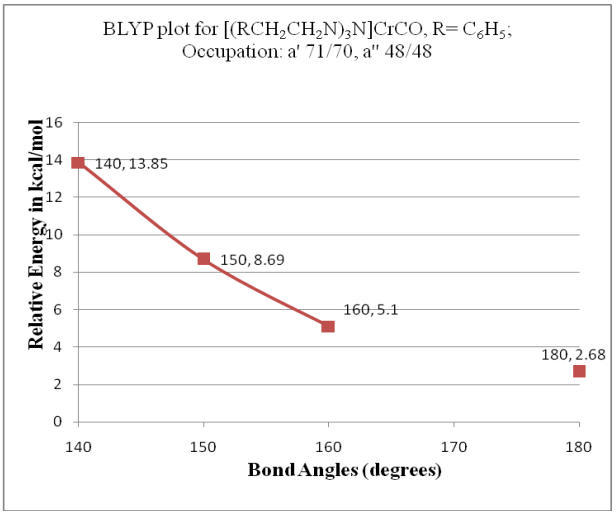

B

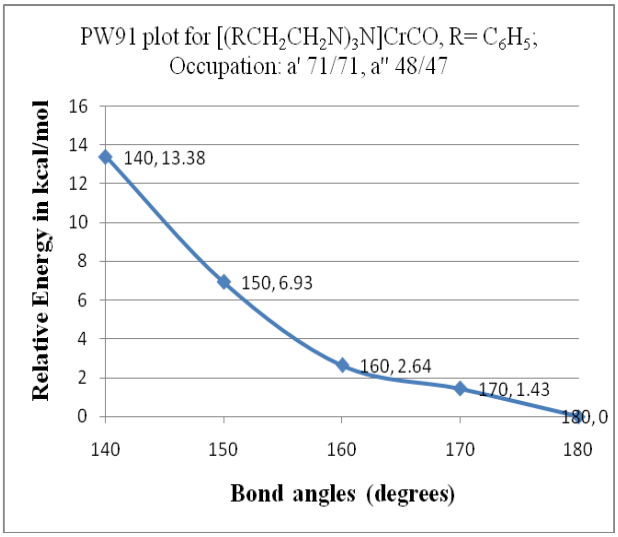

C

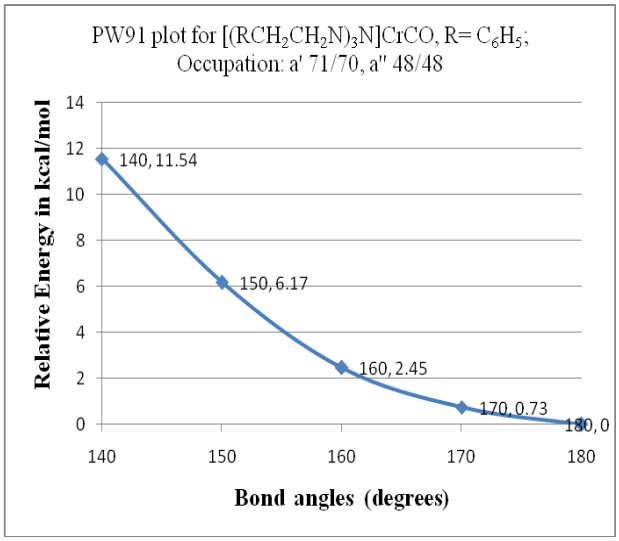

D

Figure 4.5. Shows trends in relative energy observed for some different DFT XC functional; A) BLYP functional occupation 1, B) BLYP functional occupation 2, C) PW91 functional occupation 1 and D) PW91 functional occupation 2.

4.2 Molecular Geometry Analysis

A) Bond lengths and Bond Angles Considerations

Bond Lengths

There are some observable trends in bond lengths and bond angles as the restrained angle is varied. For geometry optimizations done on the complex $[C_6H_5NCH_2CH_2]_3NCr^{III}CO$ (**1**) with the OLYP functional, there was a change in Cr-C1 bond length as the restrained bond angle was varied whereas the C-O bond length remained the same. This observation was made for both occupations of **1** where occupations 1 is a' 71/71 and a" 48/47 and occupation 2 is a' 71/70 and a" 48/47. These results have been shown in the Table 4.2 below. This trend agrees with a few results obtained from calculations done with the other XC functionals on complex **1** for its different spin occupation with the variation of the restrained angle of Cr-C-O.

Table 4.2. showing the trends in bond lengths around the Cr central atom for different occupations of the $[C_6H_5NCH_2CH_2]_3NCr^{III}CO$ complex as the restrained bond angles are varied (bond lengths are all given in Angstroms). Where N_1, N_2 and N_3 are the equatorial nitrogen of the triamidoamine ligand while N_4 is the axial nitrogen.

OLYP Bond length results for the $[C_6H_5NCH_2CH_2]_3NCr^{III}CO$ complex										
	Occupation 1: a' 71/71 and a" 48/47					Occupation 2: a' 71/70 and a" 48/48				
	140^o	150^o	160^o	170^o	180^o	140^o	150^o	160^o	170^o	180^o
Cr-C1	1.957Å	1.915Å	1.892Å	1.877Å	1.874Å	1.925Å	1.902Å	1.888Å	1.878Å	1.875Å
C1-O	1.159 Å	1.159 Å	1.159 Å	1.159 Å	1.159 Å	1.159 Å	1.159 Å	1.159 Å	1.159 Å	1.159 Å
Cr-N_1/N_3	1.926 Å	1.925 Å	1.924 Å	1.924 Å	1.925 Å	1.928 Å	1.927 Å	1.928 Å	1.908 Å	1.907 Å
Cr-N_2	1.863 Å	1.857 Å	1.852 Å	1.843 Å	1.845 Å	1.862 Å	1.857 Å	1.853 Å	1.880 Å	1.882 Å
Cr-N_4	2.191 Å	2.194 Å	2.196 Å	2.201 Å	2.200 Å	2.198 Å	2.204 Å	2.209 Å	2.203 Å	2.204 Å

Another observation made is that as the restrained bond angle of Cr-C-O is increased, the bond distance of Cr-C1 reduces which makes the structure with 180^o restrained angle to have the shortest distance of 1.874Å for occupation 1 and 1.875Å for occupation 2 which are very much different from the bond result obtained by Smythe *et al* [26] that reveals the Cr-C1 bond length to

[26] Smythe, N. C.; Schrock, R. R.; Müller,P.; Weare W. W., *Inorg. Chem.*, **2006**, 45, 1. (Supporting Information)

be 1.905Å for [HIPTN$_3$N]CrCO complex. The possible explanation for the change in the Cr-C1 bonds length with change in Cr-C-O restrained angle and the C-O bond length being constant is that the σ-donation/π-backbonding interaction of Cr and CO ligand is too weak to cause a strain on the C-O bond length. On the other hand the Cr-N4 bond directly opposite the Cr-C bond does not increase in bond length as the restrained bond angle is increased. Smythe *et al*[26] crystal data revealed a C1-O bond length of 1.142Å which is shorter than those observed here which range from 1.159Å -1.161Å. This discrepancy can be attributed to the different methods employed.

For all the calculations done, it was observed that for the three equatorial Cr-N bonds, two where always the same in length (Cr-N_1 and Cr-N_3) while one was shorter in length (Cr-N_2) and this can be attributed to the fact that at any point in time the structure strives to attend a trigonal bipyramidal shape. Smythe *et al*[26] obtained a different result for the equatorial nitrogen; where Cr-N2 was 1.874Å, Cr-N1 was 1.879Å and Cr-N3 was 1.881Å. This difference in results shows that the equatorial nitrogens of my structures very much approximate a trigonal shape compared to theirs. I believe this difference in trigonal shape approximation is due to the less displacement of the Cr central metal atom of my structures compared to theirs which might have been caused by the less sterically demanding auxiliary groups of my complexes and their difference in electron donating tendencies from the HIPT group used by Smythe *et al*.[26] Filippou et al[21,22,23] also did obtain results with all the Cr-Equatorial N (Cr-Neq) being different in bond lengths and in their case the auxiliary ligand they used was $(CH_3)_3Si$ or Me_3Si.

The results obtained for calculations with the different XC functionals and their respective spin occupation had some trends that agree with those obtained for the OLYP functional. Notwithstanding, for some of these functionals or one of their spin occupational calculation, the C-O bond lengths changes as the Cr-C-O restrained bond angle is varied but these changes do not have a constant pattern (See Table 4.3, 4.4 and 4.5 below).

Table 4.3. Gives us the bond lengths around the Cr central metal for the PW91 XC functional and its two spin occupations. The trend that confirms the OLYP result is in blue.

PW91 Bond length results for the $[C_6H_5NCH_2CH_2]_3NCr^{III}CO$ complex										
	Occupation 1: a' 71/71 and a" 48/47)					Occupation 2: a' 71/70 and a" 48/48				
	140°	150°	160°	170°	180°	140°	150°	160°	170°	180°
Cr-C1	1.952Å	1.917Å	1.897Å	1.884Å	1.882Å	1.925Å	1.904Å	1.893Å	1.883Å	1.881Å
C1-O	1.160Å	1.159Å	1.159Å	1.160Å	1.159Å	1.160Å	1.160Å	1.160Å	1.160Å	1.160Å
Cr-N1	1.915Å	1.916Å	1.915Å	1.917Å	1.915Å	1.921Å	1.921Å	1.921Å	1.904Å	1.903Å
Cr-N2	1.858Å	1.852Å	1.847Å	1.839Å	1.841Å	1.853Å	1.848Å	1.844Å	1.866Å	1.868Å
Cr-N3	1.915Å	1.916Å	1.915Å	1.917Å	1.915Å	1.921Å	1.921Å	1.921Å	1.904Å	1.903Å
Cr-N4	2.166Å	2.168Å	2.170Å	2.175Å	2.173Å	2.172Å	2.177Å	2.181Å	2.179Å	2.180Å

Table 4.4. Gives us the bond lengths around the Cr central metal for the BLYP functional and its two spin occupations.

BLYP Bond length results for the $[C_6H_5NCH_2CH_2]_3NCr^{III}CO$ complex										
	Occupation 1: a' 71/71 and a" 48/47)					Occupation 2: a' 71/70 and a" 48/48				
	140°	150°	160°	170°	180°	140°	150°	160°	170°	180°
Cr-C1	1.988Å	1.948Å	1.925Å	1.912Å	1.909Å	1.960Å	1.939Å	1.922Å		1.909Å
C1-O	1.160Å	1.160Å	1.160Å	1.161Å	1.160Å	1.161Å	1.161Å	1.161Å		1.161Å
Cr-N1	1.938Å	1.939Å	1.939Å	1.941Å	1.940Å	1.945Å	1.945Å	1.945Å		1.927Å
Cr-N2	1.885Å	1.879Å	1.873Å	1.863Å	1.866Å	1.877Å	1.872Å	1.868Å		1.894Å
Cr-N3	1.938Å	1.938Å	1.939Å	1.941Å	1.940Å	1.945Å	1.945Å	1.945Å		1.927Å
Cr-N4	2.202Å	2.204Å	2.206Å	2.211Å	2.210Å	2.209Å	2.209Å	2.218Å		2.214Å

Table 4.5. Gives us the bond lengths around the Cr central metal for the OPBE and BP86 XC functionals with the results represented only for occupation 1: a' 71/71 and a" 48/47. The trend that confirms the OLYP results is in blue.

	OPBE Bond length results for the complex **1**					BP86 Bond length results for the complex **1**			
	Occupation 1:a' 71/71 and a" 48/47)					Occupation 1: a' 71/71 and a" 48/47			
	140°	150°	160°	170°	180°	140°	150°	160°	170°
Cr-C1	1.922Å	1.885Å	1.864Å	1.849Å	1.848Å	1.954Å	1.919Å	1.898Å	1.885Å
C1-O	1.159Å	1.159Å	1.159Å	1.159Å	1.159Å	1.161Å	1.161Å	1.160Å	1.161Å
Cr-N1	1.905Å	1.906Å	1.904Å	1.905Å	1.904Å	1.919Å	1.918Å	1.919Å	1.920Å
Cr-N2	1.839Å	1.833Å	1.828Å	1.820Å	1.822Å	1.861Å	1.855Å	1.850Å	1.842Å
Cr-N3	1.905Å	1.906Å	1.904Å	1.905Å	1.904Å	1.919Å	1.918Å	1.919Å	1.920Å
Cr-N4	2.154Å	2.156Å	2.159Å	2.164Å	2.162Å	2.169Å	2.172Å	2.174Å	2.179Å

Bond Angles

Looking at the bond angles around the Cr central metal atom for the structure of complex **1** with Cr-C-O restrained bond angle of 180^{o} results, we will observe that for the different XC functionals the bond angles had the same variation patterns though the values do not very much agree. The bond angle N4-Cr-C1 for occupation 2 of the complex **1** for the different XC functionals ranged from 177^{o}-177.50^{o} while those for occupation 1 ranged from 178.64^{o}-179.42^{o} (better approximation of linearity). Which means for the case of occupation 2 the axial bond N4-Cr-C is not perpendicular to the equatorial plane as define by amido nitrogen atoms N_1-N_3. As a result, the conformation obtained from calculations with occupation 2 for the complex **1** could possibly have a distorted trigonal bipyramidal shape.

Some of the trends observed for the bond lengths are the same for the bond angles since they are all obtained from the same geometry optimizations. Table 4.6 shows that for all the functionals, the N4-Cr-N1 and N4-Cr-N3 bond angles are the same but different from the N4-Cr-N2 which is possibly linked to the conformational arrange of the structure defining a trigonal equatorial shape. This is also evident from the same bond angles of N3-Cr-N2 and N2-Cr-N1 which are different in values from the N3-Cr-N1 bond angle (larger in value). This is also seen for the angles N3-Cr-C1 and N1-Cr-C1 being the same but different from the angle N2-Cr-C1. These results give us the picture that the structure is planar or very much closer to planarity. The structural results obtained by Smythe *et al*[26], and Filippou *et al*,[21,22,23] do reveal a slight difference in all of these bond angles mention above.

Table 4.6. Observed bond angles for different DFT functionals and the two different occupations used for calculation results gotten from $[C_6H_5NCH_2CH_2]_3NCr^{III}CO$ complex.

Bond angles for XC functionals with Cr-C-O restrained angles of 180^o								
	Occupation 1: a' 71/71 and a" 48/47				Occupation 2 : a' 71/70 and a" 48/48			
Bond angles (deg)	OLYP	OPBE	BLYP	PW91	OLYP		BLYP	PW91
N4-Cr-C1	179.42	179.34	178.85	178.64	177.50		177.20	177.01
N4-Cr-N1	83.20	83.61	83.20	83.46	84.51		84.30	84.58
N4-Cr-N2	83.99	84.22	83.73	83.83	80.84		80.95	80.86
N4-Cr-N3	83.20	83.61	83.20	83.46	85.51		84.30	84.58
N3-Cr-N2	114.14	113.97	113.83	113.52	122.32		122.66	122.53
N3-Cr-N1	127.80	128.54	128.32	129.17	111.17		110.36	110.82
N2-Cr-N1	114.14	113.97	113.83	113.52	122.32		122.66	122.53
N3-Cr-C1	97.05	96.67	97.28	97.11	96.88		97.28	97.09
N2-Cr-C1	95.42	95.13	95.12	94.81	96.66		96.24	96.15
N1-Cr-C1	97.05	96.67	97.28	97.11	96.88		97.28	97.09

For all cases of the XC functionals and their different occupations presented in Table 4.6, it is observed that the phenyl groups are slightly displaced around the pocket in which the ligand CO is located. This is due to a slight distortion in the torsion angles Cr-N1-C8-C9, Cr-N3-C14-C15 and Cr-N2-C20-C21 where Cr-N2-C20-C21 angle moves away from the pocket as shown in Figure 4.6.[22]

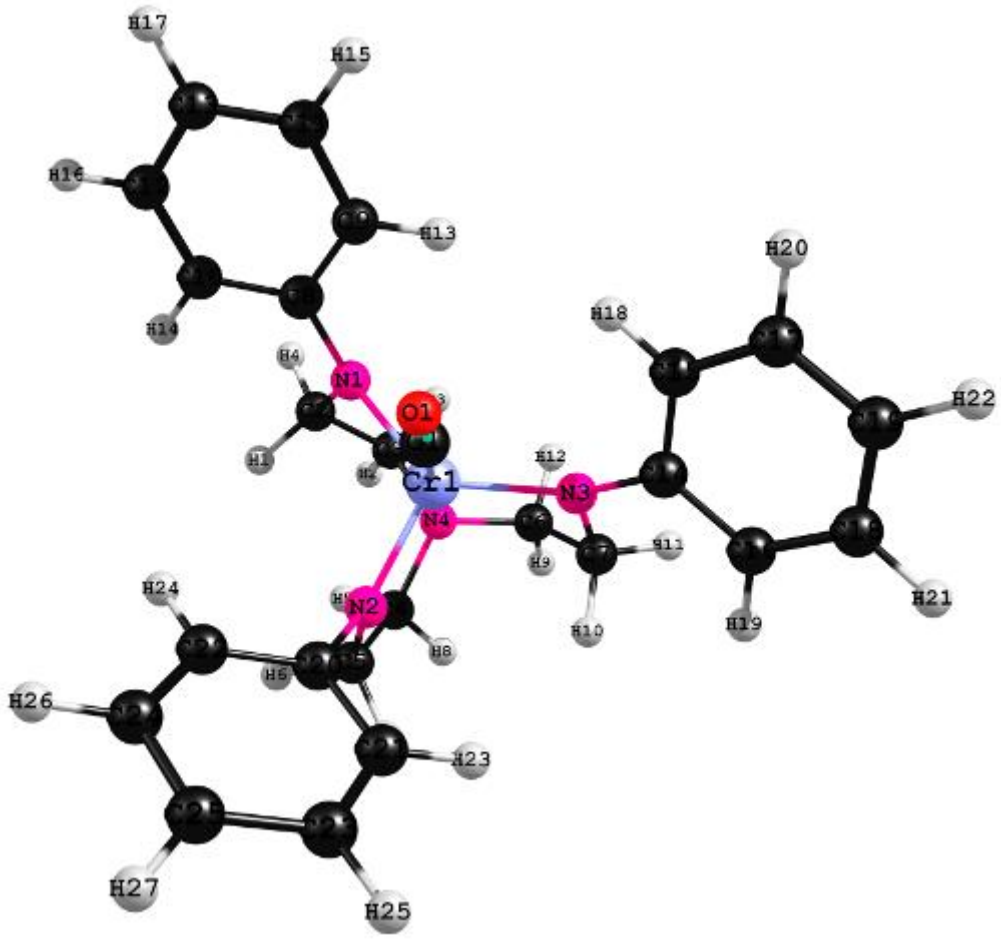

Figure 4.6. A view of the torsion angles of **1** complex with Cr-N2-C20-C21 out of the pocket.

B) Auxiliary groups Consideration

Bond Lengths

The trends found with a change in the auxiliary groups from Hydrogen (H) to methyl (CH_3) to phenyl (C_6H_5) for the DFT/OLYP calculations and their different occupations is the same as presented above as the Cr-C-O restrained angle in increased from 140^o to 180^o (this is shown in Table 4.6 and 4.7 which are being compared with the results presented in Table 4.2 above).

A notable difference in trends is that for the case where the auxiliary ligand is either H or CH_3, there is a change is the C-O bond length for their both occupations. Also, it can be seen from Tables 4.2, 4.6 and 4.7 that as the auxiliary ligand increases in size (hence more sterically

demanding), the Cr-N4 bond length increases greatly and the increase is much greater for the different occupation 2 for the respective complexes. This is probably because as the auxiliary group's electron donating tendency increases, the Cr central atom is made more electron rich hence it can donate more of its electron density to the empty π* orbital CO ligand which shortens the Cr-C1 bond and increases the Cr-N4 length.

Table 4.6. DFT/OLYP results for the bond lengths of the complex $[HNCH_2CH_2]_3NCr^{III}CO$ with hydrogen as the auxiliary ligand. These values are presented for both occupations of this complex.

	Occupation 1: a' 39/38 and a" 20/20					Occupation 2: a' 39/39 and a" 20/19				
	140°	150°	160°	170°	180°	140°	150°	160°	170°	180°
Cr-C1	1.889Å	1.870Å	1.859Å	1.853Å	1.851Å	1.920Å	1.885Å	1.864Å	1.852Å	1.847Å
C1-O	1.172Å	1.171Å	1.171Å	1.170Å	1.170Å	1.173Å	1.172Å	1.171Å	1.171Å	1.171Å
Cr-N1	1.858Å	1.857Å	1.858Å	1.858Å	1.857Å	1.860Å	1.858Å	1.857Å	1.856Å	1.855Å
Cr-N2	1.856Å	1.857Å	1.857Å	1.858Å	1.859Å	1.847Å	1.849Å	1.851Å	1.852Å	1.853Å
Cr-N3	1.858Å	1.857Å	1.858Å	1.858Å	1.857Å	1.860Å	1.858Å	1.857Å	1.856Å	1.855Å
Cr-N4	2.200Å	2.206Å	2.209Å	2.212Å	2.212Å	2.192Å	2.200Å	2.211Å	2.219Å	2.223Å

Table 4.7. DFT/OLYP results for the bond lengths of the complex $[CH_3NCH_2CH_2]_3NCr^{III}CO$ with Methyl as the auxiliary ligand. These values are presented for both occupations of this complex.

	Occupation 1: a' 46/46 and a" 25/24					Occupation 2: a' 46/47 and a" 25/25				
	140°	150°	160°	170°	180°	140°	150°	160°	170°	180°
Cr-C1	1.935Å	1.888Å	1.862Å	1.847Å	1.842Å	1.903Å	1.878Å	1.863Å	1.855Å	1.851Å
C1-O	1.172Å	1.172Å	1.172Å	1.172Å	1.172Å	1.172Å	1.172Å	1.171Å	1.171Å	1.171Å
Cr-N1	1.893Å	1.893Å	1.892Å	1.892Å	1.893Å	1.899Å	1.899Å	1.898Å	1.898Å	1.899Å
Cr-N2	1.876Å	1.868Å	1.862Å	1.857Å	1.853Å	1.869Å	1.863Å	1.859Å	1.855Å	1.853Å
Cr-N3	1.893Å	1.893Å	1.892Å	1.892Å	1.893Å	1.899Å	1.899Å	1.898Å	1.898Å	1.899Å
Cr-N4	2.202Å	2.201Å	2.201Å	2.202Å	2.203Å	2.203Å	2.206Å	2.208Å	2.210Å	2.212Å

Bond Angles

The results obtained for the bond angles for the each of these cases with different auxiliary ligand revealed the same trends presented above. Notwithstanding, there were some observed differences as the auxiliary ligand was changed. For the occupation 1 in all three cases, the N4-Cr-C1 bond angles increased from 178.37^{o}-179.42^{o} as the size of the auxiliary group increased. The reverse was observed for the occupation 2 in that as the size of the auxiliary ligand increase from hydrogen to phenyl, the N4-Cr-C1 bond angle decreased from 178.92^{o}-177.50^{o} as seen in table 4.8 below.

Another observation made is that the N3-Cr-N2 and N2-Cr-N1 bond angles (which are the same in value) decrease as the auxiliary group size increases while the N3-Cr-N1 bond angle which is usually different from the other two increased for the occupation 1 of the respective complexes. For the occupation 2 of these complexes, an irregular pattern is observed. It is of great importance to note that the difference in the N3-Cr-N1 (with same value as N3-Cr-N2) and N2-Cr-N1 bond angles becomes larger moving from hydrogen to methyl (15.45^{o} and 6.96^{o} respectively) as compared to the difference moving from methyl to phenyl (1.5^{o} and 1^{o}) auxiliary groups (this can shown in Table 4.8). These differences give a direct picture of the electron donating capacity difference between these groups which is much larger between H and CH_3 as compare to CH_3 and C_6H_5.

Table 4.8. DFT/OLYP results for the $[RNCH_2CH_2]_3NCr^{III}CO$ with a change is the auxiliary group.

	Occupation 1			Occupation 2		
	Hydrogen	Methyl	Phenyl	Hydrogen	Methyl	Phenyl
N4-Cr-C1	178.37	179.21	179.42	178.92	178.40	177.50
N4-Cr-N1	83.61	83.69	83.20	82.86	82.24	84.51
N4-Cr-N2	80.75	84.26	83.99	81.28	85.12	80.84
N4-Cr-N3	83.61	83.69	83.20	82.86	82.24	85.51
N3-Cr-N2	122.10	115.14	114.14	120.59	114.45	122.32
N3-Cr-N1	110.85	126.30	127.80	113.52	126.79	111.17
N2-Cr-N1	122.10	115.14	114.14	120.59	114.45	122.32
N3-Cr-C1	97.30	95.96	97.05	97.72	97.07	96.88
N2-Cr-C1	97.62	96.53	95.42	97.64	96.48	96.66
N1-Cr-C1	97.30	95.96	97.05	97.72	97.07	96.88

4.3 The Cr-CO orbital interaction

A) Mulliken Population Analysis

Comparison with change in auxiliary groups

Fournier[27] in his DFT calculation of CrCO and CuCO explained the bending of the Cr-CO bond in terms of the repulsion between the 5s electron pair and the metal *d* electrons and this was later studied by Gwang-Hi Jeung *et al*[28] in which they concluded that there is a weak chemical bonding involved with the CrCO species. Carrying out a mulliken population analysis for the Cr-CO bond will give us a good idea on what kind of interaction is going on.

For each $[(RNCH_2CH_2)_3N]Cr^{III}CO$ (with R=H, CH_3 and C_6H_5) complex with the respective occupations studied, a molecular symmetry of Cs was assigned. To understand the electronic structure of the Cr-CO bond and the skeleton around the triamidoamine "pocket", a mulliken population analysis was carried out. The Mulliken atomic charges were observed so as to understand the flow of electron between atoms around the said pocket especially along the apical positions (along the N4-Cr-C-O bonds).

Tables 4.9 and 4.11 shows the spin populations and atomic charge distributions of selected atoms on the $Cr^{III}CO$ triamidoamine complex for the three different auxiliary ligands and for the different DFT/XC functional respectively. It is of great importance to note that the results shown on these tables are based on the optimized geometries. The labels for the various atoms can be referred in Figure 4.6. The atomic label for the Cr, O, C1, N1, N2, N3 and N4 are the same for all complexes irrespective of the auxiliary ligand or occupation.

[27] Fournier, R. *J. Chem. Phys.*, **1993**, 98, 8041.

[28] Gwang-Hi J.; Haettel S. *Intern. J. of Q. Chem*., **1997**, 61, 547.

Table 4.9. Comparison of the DFT/OLYP Mulliken spin population densities and atomic charges *q* (these in parenthesis) for different auxiliary ligands on the $[RNCH_2CH_2]_3NCr^{III}CO$,R= H, CH_3, C_6H_5, complex shown for their respective occupations.

	Occupation 1			Occupation 2		
Atoms	Hydrogen	Methyl	Phenyl	Hydrogen	Methyl	Phenyl
Cr	1.1542 (0.9787)	1.1229 (1.0795)	1.2151 (1.0788)	1.1025 (0.9906)	1.1856 (1.0802)	1.2190 (1.0782)
C1	-0.0297 (0.2193)	-0.0379 (0.2158)	-0.0455 (0.2905)	-0.0262 (0.2158)	-0.0327 (0.2083)	-0.0488 (0.2774)
O	0.0513 (-0.3758)	0.0408 (-0.4005)	0.0419 (-0.3418)	0.0550 (-0.3774)	0.0542 (-0.3919)	0.0413 (-0.3435)
N1	-0.0658 (-0.3475)	-0.0260 (-0.6381)	-0.0441 (-0.6710)	-0.0413 (-0.3590)	-0.0596 (-0.6255)	-0.0664 (-0.6583)
N2	-0.0541 (-0.3886)	-0.0707 (-0.6117)	-0.0820 (-0.6594)	-0.0596 (-0.3602)	-0.0759 (-0.6315)	-0.0609 (-0.7031)
N3	-0.0658 (-0.3475)	-0.0260 (-0.6381)	-0.0441 (-0.6710)	-0.0413 (-0.3590)	-0.0596 (-0.6255)	-0.0664 (-0.6583)
N4	-0.0155 (-0.6108)	-0.0167 (-0.6304)	-0.0190 (-0.6449)	-0.0135 (-0.6061)	-0.0155 (-0.6261)	-0.0173 (-0.6409)

It can be observed that the spin populations and the charge on the Cr atom are larger than in the other atoms and these value increases as the auxiliary group increases in size. The same trend is observed for the charge on the C1 atom but the reverse is observed for the spin population where we see a decrease in spin population as the size of the auxiliary ligand increases. This decrease in spin population is also observed for the O atom as the auxiliary ligand increase in size. Looking at the N4 atom we also realize that there is a decrease in both spin population and atomic charge as the auxiliary ligand size increases for both occupations. This can be attributed to change in auxiliary groups with different electron donating tendencies. As the electron donation of the group increases, the more electronegative atom in the system becomes less electron rich hence lower spin population while the more electron positive atoms become more electron rich hence higher spin population.

Another observation made is that both spin population and charge values are larger for the respective occupation 2 of the triamidoamine-supported $Cr^{III}CO$ complex with the different auxiliary ligands which agrees with the bond lengths and bond angles results. The relatively high positive charges on the Cr atom and the O for the three cases makes the total charge on the Cr-O

bond relatively high which indicated that there is a high possibility of electron transfer from the Cr atom to the O atom. The net charge value for the C1-O and Cr-N4 bonds for all cases become smaller as the auxiliary group size increases from hydrogen to phenyl. This result is confirmed by an analysis of the overlap populations of some selected bonds of these complexes shown in Table 5.10. The overlap population is a measure of the shared electronic density between two atoms and a large positive value indicates that the atoms are bonded while a large negative value indicates that the atoms are in an anti-bonded state.[29,30,31]

Table 4.10. A DFT/OLYP analysis of overlap population for the triamidoamine-supported $Cr^{III}CO$ complex with different auxiliary groups on the amido nitrogens.

	Occupation 1			Occupation 2		
Bond Angles	Hydrogen	Methyl	Phenyl	Hydrogen	Methyl	Phenyl
Cr-C1	1.1245	1.0850	1.1696	1.0763	1.1529	1.1702
C1-O	0.0216	0.029	-0.0036	0.0288	0.0215	-0.0075
Cr-N1	1.0884	1.0969	1.1710	1.0612	1.1260	1.1526
Cr-N2	1.1001	1.0522	1.1331	1.0433	1.1097	1.1581
Cr-N3	1.0884	1.0969	1.1710	1.0612	1.1260	1.1526
Cr-N4	1.1387	1.1062	1.1961	1.0890	1.1701	1.2017

It is clear from these results that as the auxiliary group is changed from hydrogen to phenyl; there is an increase in electron transfer from Cr-C1 hence the strength of the bond increases where as the bonds Cr-N4 and C1-O reduces in strength. The over populations and the bond lengths agree with these results. The increase strength of the Cr-C1 bond causes the bond length to be shorter while those of Cr-N4 and C1-O become longer and the increase in length is also observed for the Cr-N1, Cr-N2 and Cr-N3 bonds.

[29] Zeng, X.; Chen, W.; Liu J. *Acta Physico-Chimica Sinica*, **2007**, 23, 192.
[30] Li, N.; Xiao, H. Y.; Zu, X. T.; Wang, L. M.; Lian J.; Ewing R. C. *J. Appl. Phys.*, **2007**, 102, 063704.
[31] Liu, Y; Li, M.; Suo Y. *Surface Science*, **2006**, 600, 5117.

Comparison with change is exchange Correlation functional

Table 5.11 below shows the spin population and charge DFT results obtained for the **1** complex with restrained Cr-C-O angle of 180^o for different XC functional calculations. These results are very much the same in trends as mentioned above. The OLYP and OPBE results agree to a lesser extend for some values while the BLYP and PW91 results agree to a lesser extend but very much different from the others. This could easily be seen from the Cr spin populations which are around 1.22 -1.25 for the OLYP and OPBE functionals while those for the BLYP and PW91 are around 1.12-1.13 and this is the same with the charge values obtained. This result agrees with the results obtained for the bond lengths and bond angles confirming the trends observed though with slightly different values.

Table 4.11. A Comparison of the DFT Mulliken spin population densities and atomic charges *q* (these in parentheses) of $[C_6H_5NCH_2CH_2]_3NCr^{III}CO$ complex with restrained Cr-C-O angle of 180^o for different XC functionals shown for their respective occupations.

	Occupation 1 (a' 71/71 and a"48/47)				Occupation 2 (a' 71/70 and a" 48/48)			
	OLYP	OPBE	BLYP	PW91	OLYP		BLYP	PW91
Cr	1.2151 (1.0788)	1.2502 (1.0671)	1.1067 (0.9550)	1.1308 (0.9107)	1.2190 (1.0782)		1.1074 (0.9569)	1.1284 (0.9162
C1	-0.0455 (0.2905)	-0.0561 (0.3018)	-0.0188 (0.2848)	-0.0249 (0.2927)	-0.0488 (0.2774)		-0.0213 (0.2683)	-0.0285 (0.2686)
O	0.0419 (-0.3418)	0.0470 (-0.3369)	0.0410 (-0.3338)	0.0462 (-0.3247)	0.0413 (-0.3435)		0.0397 (-0.3363)	0.0443 (-0.3281)
N1	-0.0441 (-0.6710)	-0.0496 (-0.6771)	-0.0274 (-0.6075)	-0.0331 (-0.5968)	-0.0664 (-0.6583)		-0.0447 (-0.5965)	-0.0497 (-0.5846)
N2	-0.0820 (-0.6594)	-0.0928 (-0.6585)	-0.0556 (-0.6057)	-0.0623 (-0.5927)	-0.0609 (-0.7031)		-0.0418 (-0.6419)	-0.0476 (-0.6336)
N3	-0.0441 (-0.6710)	-0.0496 (-0.6771)	-0.0274 (-0.6075)	-0.0331 (-0.5968)	-0.0664 (-0.6583)		-0.0447 (-0.5965)	-0.0497 (-0.5846)
N4	-0.0190 (-0.6449)	-0.0244 (-0.6573)	-0.0130 (-0.6076)	-0.0167 (-0.6047)	-0.0173 (-0.6409)		-0.0117 (-0.6042)	-0.0151 (-0.6043)

From Table 4.11 above, it can be seen that for all cases the spin population and charge values are largest for the Cr atom with a large spin population value also found around the C1 atom but the charges value is relative small. These results agree with those observe for the DFT/OLYP results obtained for the cases with the different functionals.

CHAPTER 5

CONCLUSIONS

In this work, I have carried out DFT-GGA calculations to obtain the structural and electronic properties of the complexes $[C_6H_5NCH_2CH_2]_3NCr^{III}CO$, $[CH_3NCH_2CH_2]_3Cr^{III}CO$ and $[HNCH_2CH_2]_3NCr^{III}CO$. The analysis done is based on the geometric and electronic results obtained. On the bases of the results obtained for these complexes, I draw the general conclusions that;

i) The geometric conformation obtained for all structures and all the respective occupations with restrained Cr-C1-O bond angle of 180^o is the most stable. Results obtained by Smythe *et al*[26] for the complex $[HIPTN_3N]CrCO$ also reveal that this is true. Their results predicted the Cr-C1-O bond angle to be 179.39^o

ii) The calculations reported above reveals that the bonding in these complexes is predominantly π-backbonding with spin density flowing from the d_π-orbitals (d_{xz} and d_{yz}) of the central Cr atom to the empty π* orbital of the CO ligand. An observation of the none changing C1-O bond length as the Cr-C1-O bond increases from 140^o-180^o gives us the idea that the σ-donation from the CO ligand to the metal has very little contribution to the Cr-CO bonding. Combining these two analysis from the results, I will conclude that the bonding (backbonding) in this systems occurs to a lesser extent than is the case for other transition metal-π-acceptor ligand interaction. As mentioned above, it is important to note that the slightly longer Cr-C1 bond length observed than those reported by Smythe *et al*[26] is due to the difference in methods used.

iii) As shown above in the geometry analysis of all cases involving these complexes that for bond lengths, the values obtained for Cr-N1 and Cr-N3 are the same but different from those obtained for Cr-N2 while for the bond angles, N4-Cr-N1and N4-Cr-N3 are the same but different from N4-Cr-N2; N3-Cr-N2 and N2-Cr-N1 but different from N3-Cr-N1; N3-Cr-C1 and N1-Cr-C1 are the same different from N2-Cr-C1. A possible conclusion that could be drawn is that all these structures studied are planar

with the three amido nitrogens N1, N2 and N3 defining a trigonal arrangement. If we also consider the bond angle of N4-Cr-C1 which is perpendicular to the plane and its value ranging from 177.01^{o}-179.42^{o} (closer to 180^{o}) which clearly shows that all the complexes studied in this work had a trigonal bipyramidal shape with a C_3 symmetry.

iv) On the bases of the mulliken population analysis, it can be observed as reported above that as the auxiliary group increases in electron donation, the Cr central atom becomes much more electron rich hence increasing its π-backdonation to the empty π* orbitals of the CO ligand. This was revealed in the reduction of the Cr-C1 bond length as the auxiliary group increases in electron donation and size. I do believe from these results that if the steric factor is properly taken care of, we can electronically enrich the system of these complexes to alter the geometry.

v) In future studies, I hope to further contribute to the understanding of the interaction occurring in a triamidoamine-supported Cr(III) Carbonyl complex with other computational methods. I believe that if the amido nitrogens (N1, N2 and N3) are replaced by Phosphorus atoms, we might get a more detailed understanding in the electronic chemistry going on in the complex since phosphorous can expand its octet.

REFERENCES

[1] McNaughton, R. L.; Chin, J. M.; Weare, W. W.; Schrock, R. R.; Hoffman, B. M. *J. Am. Chem. Soc.*, **2007**, 129, 3480.

[2]Smythe, N. C.; Schrock, R. R.; Muller, P.; Weare, W. W., *Inorg. Chem*., **2006**, 45, 7111.

[3]Bailar, J. C. Jr.; Emeléus, H. J.; SirNyholm, R.; Trotman-Dickenson, A. F., *Comprehensive Inorganic Chemistry*; Pergamon Press, Oxford, **1973**.

[4] Miessler, G. L. & Tarr, D. A., *Inorganic Chemistry*, Pearson Education and Pearson Prentice Hall, New Jersey, **2004**.

[5]Schrock, R. R. *Acc. Chem. Res*., **1997,** 30, 9.

[6]Schrock, R. R.; Davis, W. M.; Freundlich, J. S. *J. Am. Chem. Soc.*, **1996,** 118, 3643.

[7]Schrock, R. R. Rosenberger, C.; Seidel, S. W.; Keng-Yu S.; Davis, W. M.; Odom A. L. *J. of Org. Chem.*, **2001**, 617, 495.

[8]Weare W. W.; Hock, A. S.; Schrock, R. R.; Müller,P. *Inorg. Chem*., **2006**, 45, 9185.

[9]Yandulov, D. V.; Schrock, R. R.; Rheingold, A. L.; Ceccarelli, C.; Davis, W. M. *Inorg. Chem.*, **2003**, 42, 796.

[10] Mersmann, K.; Hauser, A.; Lehnert, N.; Tuczek, F. *Inorg. Chem*., **2006**, 45, 5044.

[11]Dobbs, D. A.; Schrock, R. R.; Davis, W. M. *lnorg. Chim. Acta*, **1997,** 263, 171.

[12]Frenking, G.; Fröhlich, N. *Chem. Rev.*, **2000,** 100, 717.

[13]Roussel, P.; Errington, W.; Kaltsoyannis, N.; Scott, P. *J. Org. Chem.* **2001,** 635, 69.

[14]Bridgeman A. J. *Inorganica Chimica Acta,* **2001,** 321, 27.

[15]Gray, G.M.; Fish, F.P.; Srivastava, D.K.; Varshney, A.; van der Woerd M. J.; and Ealick S. E. *J. Org. Chem.*, **1990.** 385, 49.

[16]Weare W. W.; Dai X.; Byrnes, M. J.; Chin, M. J.; Schrock, R. R.; Müller,P. *PNAS*, **2006**, 103, 17099.

[17]Weare W. W.; Hock, A. S.; Schrock, R. R.; Müller,P. *Inorg. Chem*., **2006**, 45, 9185.

[18]Schrock, R. R.; Greco, G. E. *Inorg. Chem.*, **2001,** 40, 3850.

19Byrnes, M. J.; Dai X.; Schrock, R. R.; Hock, A.S.; Müller,P. *Organometallics*, **2005,** 24, 4437.

[20]Filippou, A. C.; Schneider, S. *Organometallics*, **2003,** 22, 3010.

[21]Schneider, S.; Filippou, A. C. *Inorg. Chem.*, **2001,** 40, 4674.

[22]Filippou, A. C.; Schneider, S.; Ziemer B. *Eur. J. Inorg. Chem.*, **2002**, 2928.

[23]Filippou, A. C.; Schneider, S.; Schnakenburg G. *Angew. Chem. Int. Ed*., **2003**, 42, 4486.

[24]Baerends, E. J.; Branchadell, V.; Sodupe M.; Bickelhaupt, F. M.; Ziegler, T.; Rauk A.; van den Hoek, P. J.; Kleyn, A.W.; Versluis, L. ; Fan, L; Deng, L; Fischer, T.H.; Almlöf, J.; Bérces, A; van Leeuwen, R; Grüning, M.; Gritsenko, O. V.; van Gisbergen, S. J. A.; Schipper, P. R. T.; Chong, D. P.; Vosko, S. H.; Wilk, L.; Nusair, M.; Stoll, H.; Pavlidou, C. M. E.; Preuss, H.; Becke, A. D; Perdew, J. P.; Wang ,Y.; Chevary, A.; Jackson, K. A.; Pederson, M. R.; Singh, D. J.; Fiolhais, C.; Adamo, C.; Barone, V.; Burke, K.; Ernzerhof, M.; Hammer, B.; Hansen, L. B.; Norskov, J. K.; Zhang, Y.; Yang,W.; Handy, N. C.; Cohen, A. J.; Lee, C.; Parr, R. G.; Johnson, B. G.; Gill, P. M. W.; Pople, J. A.; Russo, T. V.; Martin, R. L.; Hay, P. J.; Neumann, R.; Nobes, R. H.; Hamprecht, F. A.; Tozer, D. J.; Boese, A. D.; Doltsinis, N. L.; Sprik, M.; Tsuneda, T.; Suzumura, T.; Hirao, K.; Krieger, J. B.; Chen, J.; Iafrate, G. J.; Savin, A.; Kurth, S.; Zupan, A.; Blaha, P.; van Voorhis, T.; Scuseria, G. E.; Filatov, M.; Thiel, W.; Proynov, E. I.; Sirois, S.; Salahub, D. R.; Chermette, H.; Patchkovskii, S.; Autschbach, J.; Philipsen, P. H. T.; van Lenthe, E.; Snijders, J. G.; Ros, P.; DeKock, R. L.; Boerrigter, P. M.; Hengelmolen, R.; Buijse, M. A.; Tschinke, V.; Ravenek, W.; Li, J.; Schreckenbach, G.; van Lenthe, E.; Ehlers, A. E.; Pye, C. C.; Klamt, A.; Schüürmann, G.; Jones, V.; Pascual-Ahuir, J. L.; Silla, E.; Tunon, I.; Gross, E. K. U.; Dobson, J. F.; Petersilka; Osinga, V. P.; Gritsenko, O. V.; Casida, M. E.; Jamorski, C.; Casida, K. C.; Kootstra, F.; Rosa, A.; Ricciardi, G.; Groeneveld, J. A.; Fonseca Guerra, C.; Champagne, B.; Perpète, E. A.; Robins, K. A.; Kirtman, B.; Bishop, D. M; Willets, A.; Rice, J. E.; Burland, D. M.; Shelton, D. P.; van der Avoird, A.; Wormer, P. E. S.; Bulo, R. E.; Ehlers, A. W.; Grimme, S.; Lammertsma, K.; Pauncz, R; Szabo, A.; Ostlund, N. S.; Wullen, C. V.; Wang, S. G.; Schwarz, W. H. E.; te Velde, G.; Noodleman, L.; Bickelhaupt, F. M.; Nibbering, N. M.; van Wezenbeek, E. M.; Schreckenbach, G.; Wolff, S. K; Edmiston, C.; Rüdenberg, K.; Boys, S. F;

von Niessen, W.; Hirshfeld, F. L.; Bickelhaupt, N. J. R.; van Eikema Hommes; Fonseca Guerra, C.; Handgraaf, J. W.; Kitaura, K.; Morokuma, K.; Fujimoto, H.; Osamura, J.; Minato, T.; Wolfe, S.; Mitchell, D. J.; Whangbo, M. H.; Stone, A. J. and R. W. Erskine; Bernardi, F., A. Bottoni, A. Mangini, and G. Tonachini; van den Hoek, P. J.; Watson, M. A.; Farkas, Ö.; Schlegel, H. B.; Mayer, I.; Jensen, L.; van Duijnen, P. T.; Swart, M.; Astrand, P. O.; Osted, A.; Kongsted, J.; Mikkelsen, K. V.; Michalak, A.; Nalewajski, R. F.; Mrozek, J.; Mazur, G.; Gopinathan, M. S.; Jug, K.; Wang, F.; Hirata, S.; Head-Gordon, M.; Henkelman, G.; Uberuaga, B. P.; Jonsson, H.; Vignale, G.; Kohn, W.; van Faassen, M.; de Boeij, P. L.; Berger, J. A.; Nifosi, R.; Conti, S.; Tosi, M. P.; Qian Z. X.; Vigna, G.; Stener, M.; Fronzoni, G.; de Simone, M.; van Duijnen, P. T.; Keal, T. W.; Tozer, D. J.; Xu, X.; Goddard III, W. A.; Baker, J.; Kessi, A.; Delley, B.; Swart, M.; Ehlers, A. W.; Stephens, P. J.; Devlin, F. J.; Chabalowski, C. F.; Frisch, M. J.; Reiher, M.; Salomon, O.; Hess, B. A.; Kang, J. K.; Musgrave, C. B.; Lynch, B. J.; Fast, P. L.; Harris, M.; Truhlar, D. G.; Wesolowski, T. A.; Warshel, A.; Neugebauer, J.; Jacob, C. R.; Visscher, L.; Louwerse, M. J.; Belanzoni, P.; Thomas, L. H.; Fermi, E.; von Weizsiäcker, C. F.; Lembarki, A.; Chermette, H.; Lee, H.; Wang Yue; Ou-Yang, H.; Levy, M.; Thakkar, A. J.; Efremov, E.; Ariese, F.; Gooijer, C.; Nooijen, M.; Zbiri, M.; Atanasov, M.; Daul, C.; Garcia Lastra, J. M.; Dickson, R. M.; Fan, L.; Jacobsen, H.; Swerhone, D.; Wolff, S. K.; Scuseria, G.; Buckingham, A.D.; Ducere, J. M.; Cavallo L., **ADF2006.01**, SCM, *Theoretical Chemistry*, Vrije Universiteit, Amsterdam, The Netherlands

[25]Sniatynsky, R.; Cedeño D. L. *J. Mol. Structure (Theochem)*, **2004**, 711, 123.

[26]Smythe, N. C.; Schrock, R. R.; Müller,P.; Weare W. W. *Inorg. Chem.*, **2006**, 45, 1.

(Supporting Information)

[27]Fournier, R. *J. Chem. Phys.*, **1993**, 98, 8041.

[28]Gwang-Hi J.; Haettel S. *Intern. J. of Q. Chem.*, **1997**, 61, 547.

[29]Zeng, X.; Chen, W.; Liu J. *Acta Physico-Chimica Sinica*, **2007**, 23, 192.

[30]Li, N.; Xiao, H. Y.; Zu, X. T.; Wang, L. M.; Lian J.; Ewing R. C. *J. Appl. Phys.*, **2007**,102, 063704.

[31]Liu, Y; Li, M.; Suo Y. *Surface Science*, **2006**, 600, 5117.